A MODEL - FOLLOWING DIGITAL CONTROL LAW FOR AN EBF-STOL AIRCRAFT

by

Reidar Alvestad

Thesis submitted to the Graduate Faculty of the
Virginia Polytechnic Institute and State University
in partial fulfillment of the requirements for the degree of

MASTER OF SCIENCE

in

Electrical Engineering

APPROVED:

Dr. L. Hasdorff, Chairman

Dr. L. L. Grigsby

Dr. F. H. Lutze, Jr.

August, 1972

Blacksburg, Virginia

ACKNOWLEDGMENTS

The author wishes to thank for suggesting this project and for his guidance during the initial stages.

was very helpful in obtaining a hybird simulation of the aircraft used in this study.

Special thanks are extended to who was instrumental in the interpretation and proper use of the aerodynamic data and who also on many occasions helped to bring the aerospace aspects into focus.

Thanks must also go to for his guidance during the important final phase of the project during which workable results were obtained.

The author is very grateful to his wife who provided much encouragement and moral support during this extended period.

This research was sponsored by the NASA-Langley Research Center under contract

TABLE OF CONTENTS

LIST OF FIGURES

LIST OF FIGURES (Continued)

LIST OF TABLES

GLOSSARY

Term	Definition	Units
C_D	Drag coefficient	
C_L	Lift coefficient	
C_M	Moment coefficient	
C_T	Thrust coefficient	
D	Aerodynamic drag	pounds
I_y	Moment of inertia about Y axis	slugs · square feet
L	Aerodynamic lift	pounds
M_y	Pitching moment about Y axis	foot pounds
S	Wing area	square feet
V	Velocity	feet per second
$\bar{c}$	Mean aerodynamic chord	feet
g	Acceleration of gravity	feet per second squared
m	Mass of aircraft	slugs
q	Pitch rate	radians per second
$\bar{q}$	Dynamic pressure	pounds per square foot
α	Angle of attack	radians
γ	Flight path angle	radians
θ	Attitude angle	radians
δ_e	Elevator deflection	radians
δ_f	Flap deflection	radians
ρ	Static air density	slugs per foot cubed

GLOSSARY (Continued)

Term	Definition	Units
C_{L_T}	Partial change in C_L w.r.t. change in C_T	
C_{D_T}	Partial change in C_D w.r.t. change in C_T	
C_{M_q}	Partial change in C_M w.r.t. change in $\frac{q\bar{c}}{2V_0}$	
C_{M_T}	Partial change in C_M w.r.t. change in C_T	
C_{L_α}	Partial change in C_L w.r.t. change in α	
C_{D_α}	Partial change in C_D w.r.t. change in α	
C_{M_α}	Partial change in C_M w.r.t. change in α	
$C_{L_{\delta_e}}$	Partial change in C_L w.r.t. change in δ_e	
$C_{D_{\delta_e}}$	Partial change in C_D w.r.t. change in δ_e	
$C_{M_{\dot{\delta}_e}}$	Partial change in C_M w.r.t. change in δ_e	
$C_{L_{\delta_f}}$	Partial change in C_L w.r.t. change in δ_f	

GLOSSARY (Continued)

Term	Definition	Units
$C_{D_{\delta_f}}$	Partial change in C_D w.r.t. change in δ_f	
$C_{M_{\delta_f}}$	Partial change in C_M w.r.t. change in δ_f	

CHAPTER I

INTRODUCTION

In the past few years, a considerable amount of research effort has been directed towards alleviating the congestion at our major airports. This research has lead to the consideration of utilizing vertical and/or short take-off and landing (V/STOL) aircraft as a means of solution. Currently, the emphasis is on the development of STOL aircraft since the objectives seem to be closer at hand. One particular design of this type which shows considerable promise makes use of the jet engine exhaust gases impinging on a deflected surface of the wing at low speeds to generate additional aerodynamic lifting forces which are not present on conventional aircraft. The additional lifting force gives the aircraft its short take-off and landing capability. This type of aircraft is called an externally blown flap, STOL vehicle or EBF-STOL.

The objective of this thesis is to design a digital controller for an EBF-STOL aircraft that will enable the pilot to control the aircraft and have the same handling qualities throughout the entire flight regime. The handling qualities describe the response of the aircraft to pilot commands and are generally dictated by the short-period mode of the system matric. The digital controller acts to augment the pilot commands when necessary such that these conditions are satisfied.

Usually, the approach taken in designing a controller is to linearize the aircraft equations of motion about some reference flight condition and then apply linear optimal-control theory to determine the feedback and feedforward gains so that the flying quality criteria are satisfied. The feedback gains provide a means of closing the control loop around each of the plant state variables while the feedforward gains multiply the states of and inputs to some desirable reference model, thus making it a prefilter to the plant. For conventional aircraft, these gains are usually held constant over the entire flight regime. However, the non-linear aerodynamics of the EBF-STOL aircraft do not allow such an easy solution. In particular the feedback and feedforward gains must be changed almost continually with flight condition in order to satisfy the flying quality specifications.

This thesis considers a model-following scheme which generates constant gains over piecewise linear portions of the aerodynamic data. The reference model used for this study is that of the B-26 aircraft. The problem is then formulated as a discrete linear regulator problem and the associated matrix Riccati equation is solved to obtain the feedback and feedforward gains which cause the states of the linearized plant to follow those of the desirable model.

As a preliminary to this study, an analog hybrid simulation of the longitudinal equations of motion was implemented at the NASA-LANGLEY Research Center, Hampton, Virginia. In choosing a

design technique, future implementation on the hybird system had to be considered. For this reason, the system equations are discretized from the start which facilitates use of the discrete matrix Riccati equation.

CHAPTER II

DERIVATION OF THE LINEAR SYSTEM EQUATIONS

2.1 Introduction

In order to utilize the state variable techniques of Ogata [1], and the linear regulator theory presented in Kirk [2], the plant must be represented in the form

$$\dot{x} = Ax + Bu \tag{2.1}$$

with x an (n x 1) vector of the state variables, u an (m x 1) vector of the control inputs, A an (n x n) constant matrix, and B an (n x m) constant matrix. A is referred to as the system matrix and B the control matrix.

Only the time-invariant case is considered since it assures constant gains which are easier to implement. However, the equations of motion of the EBF-STOL vehicle are nonlinear as well as time-varying. Therefore, some linearization technique must be used. The equations are linearized using small perturbations about a reference flight condition. The system and control matrices are made piecewise constant by considering piecewise constant portions of the aerodynamic data. Linearization of the aerodynamic data is discussed in Appendix A.

2.2 Aircraft Equations of Motion

For this study, only the equations in the longitudinal plane are considered, which assumes a sufficient decoupling of the lateral and longitudinal motions. This assumption is valid according to Etkin [3] provided: there exists a plane of symmetry; the equations are linearized; the rotor gyroscopic effects and all aerodynamic cross-coupling are neglected.

Figure 2.1 shows the orientation of the aircraft with respect to ground. The equations of motion are obtained by summing forces in the X and Z directions and by summing moments about the Y axis. The forces due to thrust are included in the drag and lift terms and therefore do not appear explicitly in the equations of motion.

$$\Sigma F_x = m\dot{V} = -D - mg\mathrm{Sin}\gamma \tag{2.2}$$

$$\Sigma F_z = mV\dot{\gamma} = L - mg\mathrm{Cos}\gamma \tag{2.3}$$

$$\Sigma M_y = I_y\dot{q} = M_y \tag{2.4}$$

The aerodynamic terms can be written as functions of the aerodynamic coefficients.

$$L = \bar{q}\ S\ C_L \tag{2.5}$$

$$D = \bar{q}\ S\ C_D \tag{2.6}$$

$$M_y = \bar{q}\ S\ \bar{c}\ C_M \tag{2.7}$$

where C_L, C_D, and C_M are the lift, drag, and moment coefficients respectively. The equations of motion then become

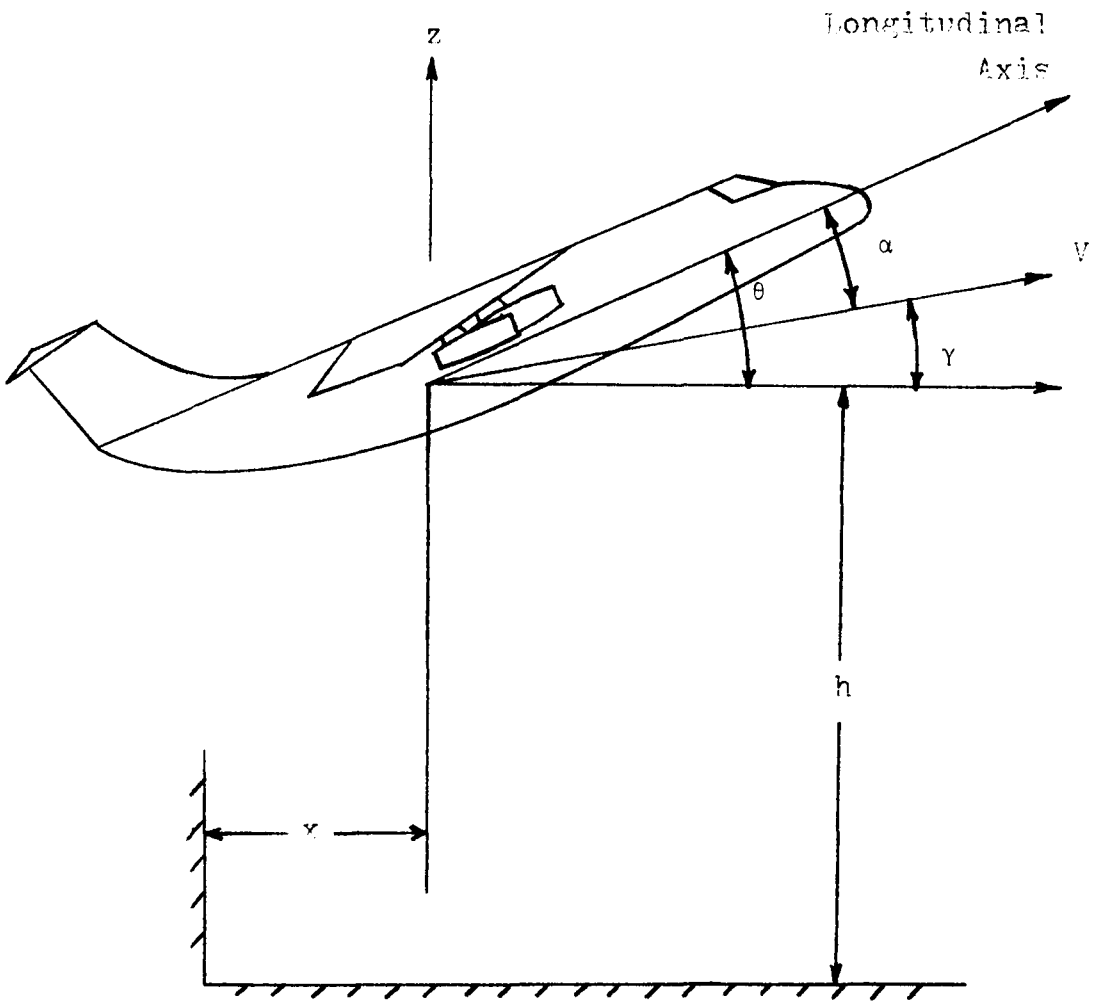

Figure 2.1 Aircraft Orientation

$$\dot{V} = -\frac{\bar{q}SC_D}{m} - g\mathrm{Sin}\gamma \tag{2.8}$$

$$\dot{\gamma} = \frac{\bar{q}SC_L}{mV} - \frac{g\mathrm{Cos}\gamma}{V} \tag{2.9}$$

$$\dot{q} = \frac{\bar{q}S\bar{c}C_M}{Iy} \tag{2.10}$$

$$\dot{\theta} = q \tag{2.11}$$

$$\text{where } \bar{q} = \tfrac{1}{2}\rho V^2 \tag{2.12}$$

The equations of motion are time-varying functions of the aerodynamic force coefficients (C_L, C_D, and C_M). Each of these coefficients is a function of several variables (α, C_T, δ_e, δ_f) which can be expanded in a Taylor series (retaining only the first order terms).

$$C_D = C_{D_0} + C_{D_\alpha}\Delta\alpha + C_{D_T}\Delta C_T + C_{D_{\delta_e}}\Delta\delta e + C_{D_{\delta_f}}\Delta\delta f$$

$$C_L = C_{L_0} + C_{L_\alpha}\Delta\alpha + C_{L_T}\Delta C_T + C_{L_{\delta_e}}\Delta\delta_e + C_{L_{\delta_f}}\Delta\delta f \tag{2.13}$$

$$C_M = C_{M_0} + C_{M_\alpha}\Delta\alpha + C_{M_T}\Delta C_T + C_{M_{\delta_e}}\Delta\delta_e + C_{M_{\delta_f}}\Delta\delta f$$

$$+ C_{M_q}\Delta q$$

where the subscript (0) is used to indicate the nominal value. The other subscripted terms are stability and control derivatives which are discussed in Appendix A.

The system has four state variables (V, γ, θ, q) and two control variables (δ_e, C_T). For the type of STOL aircraft used in this study, the flaps are not included as a control variable. Instead, the flaps have three possible positions: zero degrees, 15/30 degrees (half), and 30/60 degrees (full). As a result, the terms involving $\Delta\delta_f$ in Equation 2.13 are deleted.

2.3 Determination of the Nominal Values

The flight condition considered in this thesis is horizontal steady flight in the longitudinal plane. The nominal values of the state variables are not determined such that this condition is satisfied.

From Equation (2.8)

$$\dot{V}_0 = 0 = -\frac{\bar{q}SC_{D_0}}{m} - g\sin\gamma_0 \tag{2.14}$$

Horizontal flight implies

$$\gamma_0 = \theta_0 = 0$$

and therefore

$$C_{D_0} = 0$$

Since the effect of thrust is accounted for in the force coefficients, this equation states that drag is equal to thrust in steady flight.

$$\dot{\gamma}_0 = 0 = \frac{\bar{q}SC_L}{m} - \frac{g\cos\gamma_0}{V_0} \tag{2.15}$$

or $$C_{L_0} = \frac{W}{\bar{q}S} \tag{2.16}$$

From Equation (2.10)

$$\dot{q}_0 = \frac{\bar{q}S\bar{c}C_M}{Iy} = 0 \tag{2.17}$$

Therefore

$$C_{M_0} = 0.$$

The nominal constants to be used in the plant equations are

$$C_{D_0} = 0$$

$$C_{L_0} = 2.57$$

$$C_{M_0} = 0$$

$$V_0 = 150$$

$$\gamma_0 = 0$$

2.4 The Linearized Equations of Motion

As already stated, in order to use modern control theory, the system must be in the form of a linear state model. This is accomplished by perturbing the dynamic variables about their respective nominal values. These variables then become

$$V_0 + \Delta V$$

$$\gamma_0 + \Delta\gamma$$

$$\theta_0 + \Delta\theta$$

$$q_0 + \Delta q$$

and the control variables are

$$\delta_e = \delta_{e_0} + \Delta\delta_e$$

$$C_T = C_{T_0} + \Delta C_T$$

Substituting the above into Equations (2.8), (2.9), (2.10), and (2.11) yields

$$\dot{V}_0 + \Delta\dot{V} = -\frac{\rho S}{2m}(V_0 + \Delta V)^2 C_D - g\text{Sin}(\gamma_0 + \Delta\gamma) \tag{2.18}$$

$$\dot{\gamma}_0 + \Delta\dot{\gamma} = \frac{\rho S}{2m}(V_o + \Delta V)C_L - g\cos(\gamma_0 + \Delta\gamma) \tag{2.19}$$

$$\dot{q}_0 + \Delta\dot{q} = \frac{\rho s\bar{c}}{2Iy}(V_0 + \Delta V)^2 C_M \tag{2.20}$$

$$\dot{\theta}_0 + \Delta\dot{\theta} = q + \Delta q \tag{2.21}$$

The aerodynamic coefficients above (C_D, C_L, C_M) are functions of several variables as described by Equation (2.13). Making this substitution and using the trigonometric identities

$$\text{Sin}(x + y) = \text{Sinxcosy} + \text{cosxsiny}$$

$$\cos(x + y) = \text{cosxcosy} - \text{sinxsiny} \tag{2.22}$$

and remembering that for small values of x

$$\text{Sinx} = x$$

$$\text{cosx} = 1$$

the system equations are reduced to

$$\Delta\dot{V} = -\frac{\rho SV_0^2}{2m}\left(C_{D_\alpha}\Delta\alpha + C_{D_T}\Delta C_T + C_{D_{\delta_f}}\Delta_{\delta_f} + C_{D_{\delta_e}}\Delta_{\delta_e}\right)$$

$$-\frac{\rho SV_0}{m} C_{D_0}\Delta V - g(\cos\gamma_0)\,\Delta\gamma \tag{2.23}$$

$$\Delta\dot{\gamma} = \frac{\rho S}{2m}\left[V_0\left(C_{L_\alpha}\Delta\alpha + C_{L_T}\Delta C_T + C_{L_{\delta_f}}\Delta_{\delta_f} + C_{L_{\delta_e}}\Delta_{\delta_e}\right)\right.$$

$$\left. + C_{L_0}\Delta V\right] + g\left(\frac{\sin\gamma_0}{V_0}\Delta\gamma + \frac{\cos\gamma_0}{V_0^2}\Delta V\right) \tag{2.24}$$

$$\Delta\dot{\theta} = \Delta q \tag{2.25}$$

$$\Delta q = \frac{\rho s\bar{c}}{2Iy}\left[V_0^2\left(C_{M_\alpha}\Delta\alpha + C_{M_T}\Delta C_T + C_{M_{\delta_f}}\Delta_{\delta_f} + C_{M_{\delta_e}}\Delta_{\delta_e}\right.\right.$$

$$\left.\left. + \frac{\bar{c}}{2V_0} C_{M_q}\Delta q\right) + 2V_0 C_{M_0}\Delta V\right] \tag{2.26}$$

The equations can now be put in the form of Equation (2.1) using the kinematic relation

$$\Delta\alpha = \Delta\theta - \Delta\gamma$$

and letting

$$K1 = \frac{\rho sV_0^2}{2m}$$

$$K2 = \frac{\rho s V_0}{2m}$$

$$K3 = \frac{\rho s \bar{c} V_0^2}{2I_y}$$

for simplicity. Equation (2.27) is the resulting state model in the perturbation variables.

2.5 Determination of a Desirable Model

As stated in the Introduction, the response of the aircraft must satisfy certain flying qualities. These flying qualities are determined to a large extent by the phugoid and short period modes of the aircraft. It is desirable for the phugoid mode to have a long period and little damping, while the short-period mode should be rapid with heavy damping. The characteristics of the two modes are determined by the system matrix. Due to the special aerodynamics of the EBF-STOL vehicle, a perfect system matrix which meets all of the flying qualities specifications and also leads to good illustrative results is not available.

Instead, the model chosen for this study is that of a B-26 aircraft which is determined from the study done by Tyler [5]. This model (Equation 2.28) will serve well to demonstrate the control algorithm.

$$\begin{bmatrix} \Delta\dot{V} \\ \Delta\dot{\gamma} \\ \Delta\dot{\theta} \\ \Delta\dot{q} \end{bmatrix} = \begin{bmatrix} -2K2\ C_{D_0} & C_{D_\alpha} K1 - g\cos\gamma_0 & -K1C_{D_\alpha} & 0 \\ \frac{K2C_{L_0}}{V_0} + \frac{g\cos\gamma_0}{V_0^2} & \frac{g\sin\gamma_0}{V_0} - K2C_{L_\alpha} & K2C_{L_\alpha} & 0 \\ 0 & 0 & 0 & 1 \\ \frac{2K3}{V_0}\ C_{M_0} & -K3C_{M_\alpha} & K3C_{M_\alpha} & \frac{\bar{c}K_3}{2V_0} C_{M_q} \end{bmatrix} \begin{bmatrix} \Delta V \\ \Delta\gamma \\ \Delta\theta \\ \Delta q \end{bmatrix}$$

$$+ \begin{bmatrix} -K1C_{D_{\delta_e}} & -K1C_{D_T} \\ K2C_{L_{\delta_e}} & K2C_{L_T} \\ 0 & 0 \\ K3C_{M_{\delta_e}} & K3C_{M_T} \end{bmatrix} \begin{bmatrix} \Delta_{\delta_e} \\ \Delta C_T \end{bmatrix}$$

Equation (2.27)

$$\begin{bmatrix} \Delta \dot{V} \\ \Delta \dot{\gamma} \\ \Delta \dot{\theta} \\ \Delta \dot{q} \end{bmatrix} = \begin{bmatrix} -.038 & 1.32 & -33.52 & 0 \\ .002 & -.499 & .476 & 0 \\ 0 & 0 & 0 & 1 \\ .001 & .522 & -.532 & -1.09 \end{bmatrix} \begin{bmatrix} \Delta V \\ \Delta \gamma \\ \Delta \theta \\ \Delta q \end{bmatrix}$$

$$+ \begin{bmatrix} 0 & 5.65 \\ .072 & .01 \\ 0 & 0 \\ .855 & .004 \end{bmatrix} \begin{bmatrix} \Delta_{\delta_e} \\ \\ \Delta C_T \end{bmatrix} \qquad \text{(Equation 2.28)}$$

CHAPTER III

THE MODEL-FOLLOWING SCHEME

3.1 Background

The concepts of model-following, model-reference, and adaptive control systems are well established in the literature. Tyler [5] and Erzberger [6] have applied linear optimal-control theory to the two basic model-following concepts; implicit model-following and real model-following. In the former, the model is incorporated in the cost function only, which is then minimized to determine the feedback gains.

In real model-following, the model system matrix is incorporated in the overall system. This is done by writing it as an uncontrollable part of the state equations. The dimension of the state vector is thus increased to 2n. The technique used in this study is a modification of real model-following in that both the model system and control matrices are included in the state equations. This allows simulation of command inputs to the model. Real model-following was chosen because it was felt that it could better correct for random disturbances than implicit model-following and it was also seen that this feature could be easily and cheaply implemented by hybird simulation.

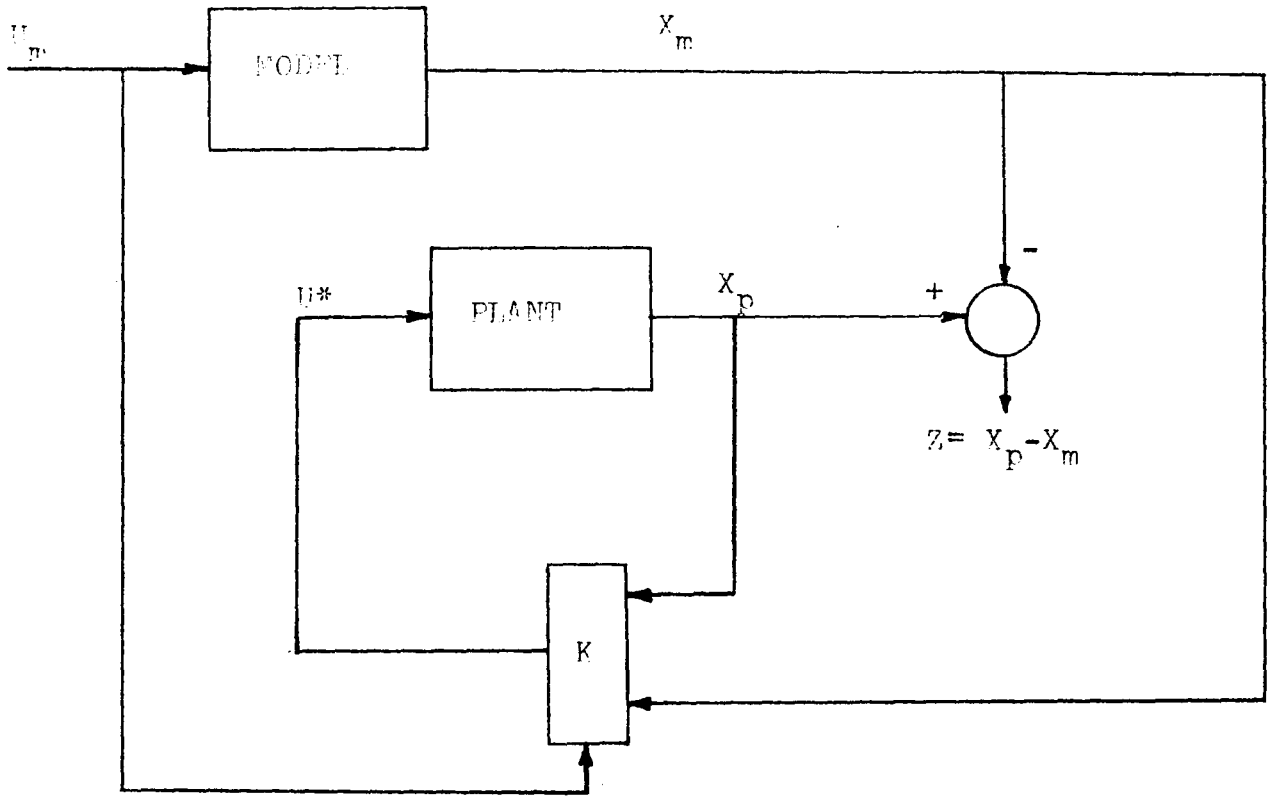

Figure 3.1 The Model-Following Scheme

3.2 Determination of the Control Law

It is assumed that a desirable model for the given system can be found which satisfies the following conditions:

1) It possesses the desired flying qualities,

2) It is controllable and stable, and

3) It can be represented in state variable form.

The model-following scheme is shown in Figure 3.1 where U_m are the pilot inputs to the model, U^* is the optimal control law, X_m is the model state vector, X_p is the plant state vector, and Z is the difference between plant and model states which can be written as

$$Z = X_p - X_m \tag{3.1}$$

Then as Z approaches a minimum the response of the plant approaches that of the model. From Kirk [2], the cost function needed to find an optimal, feedback control law is of the form

$$J = \int_0^\infty (Z^T Q Z + U^T R U)\, dt \tag{3.2}$$

with Z an (n x n) positive semi-definite matrix and R an (m x m) positive definite matrix.

The inputs to the model, U_m are formulated as state variables to give

$$\begin{bmatrix} \dot{X}_p \\ \dot{X}_m \\ \dot{U}_m \end{bmatrix} = \begin{bmatrix} A_p & 0 & 0 \\ 0 & A_m & B_m \\ 0 & 0 & 0 \end{bmatrix} \begin{bmatrix} X_p \\ X_m \\ U_m \end{bmatrix} + \begin{bmatrix} B_p \\ 0 \\ 0 \end{bmatrix} [U]$$

where U=U*, which is to be determined.

Equation (3.1) can be written as

$$Z = [H] \begin{bmatrix} X_p \\ X_m \\ U_m \end{bmatrix} = H \tilde{X} \tag{3.3}$$

where H is an [n x (2n + m)] matrix and $\tilde{X}$ is the overall system vector of order (2n + m). Then the first term of Equation (3.2) becomes

$$Z^T Q Z = (H \tilde{X})^T Q(H \tilde{X}) = \tilde{X}^T H^T Q H \tilde{X} \tag{3.4}$$

Defining

$$\tilde{Q} = H^T Q H \tag{3.5}$$

the cost function can be written as

$$J = \int_0^t (\tilde{X}^T \tilde{Q} \tilde{X} + U^T R U) \, dt \tag{3.6}$$

Using the homogeneous continuous-time state model (Equation 3.7) we can calculate the transition matrix Φ,

$$\begin{bmatrix} \dot{X}_p \\ \dot{X}_m \\ \dot{U}_m \\ \dot{U} \end{bmatrix} = \begin{bmatrix} A_p & 0 & 0 & B_p \\ 0 & A_m & B_m & 0 \\ 0 & 0 & 0 & 0 \\ 0 & 0 & 0 & 0 \end{bmatrix} \begin{bmatrix} X_p \\ X_m \\ U_m \\ U \end{bmatrix} \tag{3.7}$$

which can be represented by

$$\dot{Y} = A Y \tag{3.8}$$

with Y a vector of order (2n + 2m) and A is a square matrix of order (2n + 2m).

The transition matrix for the system of Equation (3.8) can be written in partitioned form as,

$$\Phi = \left[\begin{array}{c|c} \phi & \Psi \\ \hline 0 & I \end{array}\right] \tag{3.9}$$

from which the discrete state model is formulated as

$$\tilde{X}\ (k + 1) = \phi\ \tilde{X}(k) + \Psi U(k) \tag{3.10}$$

with ϕ a square matrix of order (2n + m) and Ψ a [(2n + m) x m] matrix with $\tilde{X} = \begin{bmatrix} X_p \\ X_m \\ U_m \end{bmatrix}$ a (2n + m) vector.

From Sage [7], the Riccati equation for a discrete system

$$x(k + 1) = Ax(k) + Bu(k)$$

with cost criterion

$$J = \sum_{k=1}^{n-1} (X^T(k)QX(k) + U^T(k)\ R\ U\ (k))$$

is

$$K(n) = Q + A^T\ [K(n + 1) + B\ R^{-1}\ B^T]^{-1}\ A \tag{3.11}$$

where K is the (m x n) matrix of Kalman gains. For purposes of digital computer computation the gains are calculated from the following algorithm which is taken from Kirk [2].

$$K(n - k) = - [R + B^T P(k - 1) B]^{-1} B^T P(k - 1) A \tag{3.12}$$

$$P(k) = [A + B K(n - k)]^T P(k - 1) [A + B K(n - k)]$$

$$+ K^T(n - k) R K(n - k) + Q \tag{3.13}$$

where A, B, R, and Q are constant and $A=\emptyset$. $B=\Psi$. $Q=\tilde{Q}$.

The algebraic matrix equations are solved backwards in time for large n, and k increasing from zero to n with the initial condition

$$P(0) = \tilde{Q}. \tag{3.14}$$

Since the control problem is formulated as a linear regulator the optimal control law is time-invariant under the following conditions:

1) The system is completely controllable and time-invariant.

2) R and Q are constant matrices, and

3) A final state is not specified in the cost function.

Therefore, since these conditions are satisfied K approaches a steady state value for a given n and ε such that

$$K(n) - K(n - 1) \leq \varepsilon \tag{3.15}$$

where ε is the acceptable error and n depends on ε.

The optimal control vector then becomes

$$U^*(k) = K \tilde{X}(k) \tag{3.16}$$

where K is the steady state value of the gain matrix, i.e.

$$K = \lim_{k \to \infty} K(k)$$

Equation (3.10) can now be written as

$$\tilde{X}(k+1) = (\emptyset + \Psi K)\,\tilde{X}(k) \tag{3.17}$$

which is solved recursively to obtain the time response.

CHAPTER IV

RESULTS AND RECOMMENDATIONS

4.1 Introduction

In this study, results are obtained for the half-flap configuration linearized about a single point of the flight regime using small perturbation theory. The nominal values are calculated in Section 2.3 and the values used for the stability and control derivatives are given in Table I.

The closed-loop time response of the model and plant states are presented for a 5^{o} step input to the elevator and for a 0.25 step input to the thrust coefficient. Results are also obtained for a filtered gaussian input to each control variable. These inputs are the pilot commands to the model which are simulated as state variables, thus allowing them to be represented as initial conditions. For the elevator input a gaussian signal with zero mean and a standard deviation of one-tenth is used. Since the commanded thrust coefficient must be positive the gaussian signal used for this control has mean and standard deviation equal to one-tenth, which provides an acceptable command signal.

In order to simplify the discussion and labeling of the graphs, each input is considered a different case. The four cases are shown in Table II.

4.2 Discussion of the Results

The cost function (Equation 3.2) contains two diagonal weighting matrices, Q and R. If Q is high with respect to R, then the difference between plant and model states (Equation 3.1) is weighted more heavily than the controls in the calculation of the gain matrix K. In obtaining the closed-loop time response, R is held constant at unity while several runs are made for different values of Q. Each response curve presented in this chapter is labeled with the diagonal elements of the Q matrix. For simplicity and readability all other entries of this weighting matrix are assumed to be zero.

It is highly desirable to use the same gain matrix for inputs to either of the control variables. These inputs to the model are included in the overall system state vector $\tilde{X}$ (see Section 3.2). The Riccati algorithm is independent of this vector and therefore the gain matrix K will be independent of the control variable excited.

However, using the same gain matrix when exciting either input does not guarantee that the quality of model-following will be acceptable in both cases. This problem was encountered in the present study, where it was found that good model-following was more easily obtainable for Case I than for Case II. Also, velocity was the easiest of the variables to match to the model, while attitude angle proved to be the most difficult.

For Case I, good results were obtained with Q = [10, 10, 10, 10], however, this same value of Q provided unacceptable results for Case

TABLE I

Stability and Control Derivatives for the

Half-Flap Configuration

Derivative	Value
C_{L_α}	6.3
C_{D_α}	.57
C_{M_α}	.57
C_{L_T}	.8
C_{D_T}	-.4
C_{M_T}	-.2
$C_{L_{\delta_e}}$	.02
$C_{D_{\delta_e}}$	-.0056
$C_{M_{\delta_e}}$	-.087
$C_{M_q}\left(\frac{\bar{c}}{2V_0}\right)$	-1.176

TABLE II

Input Signals for which Results

are Obtained

Case	Input Signal
I	5^{o} step input to elevator
II	0.25 step input to thrust coefficient
III	Filtered gaussian input to elevator
IV	Filtered gaussian input to thrust coefficient

II as can be seen from Figures 4.6 and 4.7. Therefore, considerable trial and error was necessary in order to find a Q that would allow use of the same gain matrix for all cases.

Figures 4.1, 4.2, 4.3, and 4.4 show the response of the state variables for Case I. Each figure contains three curves:

1) The time response of the model state variables,
2) The time response of the corresponding plant state variables for Q = [10, 10, 10, 10], and
3) The time response of the corresponding plant state variables for Q = [10, 10^5, 10^5, 10^4].

Figures 4.5, 4.6, 4.7, and 4.8 provide the same information for Case II.

Figures 4.9 and 4.10 show the required plant inputs for Case I and Case II respectively. In each case, these inputs constitute the control law of Equation (3.16).

Results are obtained next for a filtered gaussian input to the elevator (Case III) and the thrust coefficient (Case IV). In these two cases, the plant response is plotted for only one value of Q, which is [10, 10^5, 10^5, 10^4].

Figures 4.11, 4.12, 4.13, and 4.14 show the response of the state variables for Case III while Figures 4.15, 4.16, 4.17, and 4.18 give the responses for Case IV.

Figures 4.19 and 4.20 show the required plant input signals for Case III and Case IV respectively.

TABLE III

Gain and Weighting Matrices

Q	Gain Matrix
[10, 10, 10, 10]	$\begin{bmatrix} .138 & 2.04 & 5.63 & 3.00 & -.135 & -1.8 & -5.87 \\ -1.54 & 5.02 & 2.13 & 3.70 & 1.54 & .108 & -7.26 \\ & & -4.86 & -3.22 & 1.02 & & \\ & & -.915 & -.290 & 1.23 & & \end{bmatrix}$
$[10, 10^5, 10^5, 10^4]$	$\begin{bmatrix} .015 & 22.4 & 33.4 & 11.1 & .0005 & -21.6 & -34.6 \\ -.717 & -80.3 & -10.3 & -2.33 & .704 & 82.6 & 7.96 \\ & & -13.5 & -7.17 & 1.72 & & \\ & & 2.61 & 1.93 & .256 & & \end{bmatrix}$

The filtered gaussian signal applied to the elevator (Case III) is shown in Figure 4.21. This signal was properly scaled to maintain the elevator deflection within $\pm 10^{o}$. The dynamic system used as a filter for the gaussian signal is as follows:

$$\begin{bmatrix} X_1(k+1) \\ X_2(k+1) \\ X_3(k+1) \end{bmatrix} = \begin{bmatrix} .95 & 0 & 0 \\ -.01 & .95 & 0 \\ 0 & -.01 & .95 \end{bmatrix} \begin{bmatrix} X_1(k) \\ X_2(k) \\ X_3(k) \end{bmatrix} + \begin{bmatrix} -.01 \\ 0 \\ 0 \end{bmatrix} U(k)$$

where U(k) is the gaussian input.

Figure 4.22 shows the filtered gaussian input applied to the thrust coefficient (Case IV).

The gain matrices obtained for the two values of Q are presented in Table III. The corresponding state vector is

$$[V_p \quad \gamma_p \quad \theta_p \quad q_p \quad V_m \quad \gamma_m \quad \theta_m \quad q_m \quad \delta_e \quad C_T]^T$$

where the subscripts (p) and (m) denote plant and model states respectively.

All response curves shown are plotted for the perturbation variables.

4.3 Recommendations for Further Study

The work presented in this thesis is intended only as an initial phase of the continuing project involving the EBF-STOL aircraft. It is hoped that this study will provide the ground work necessary to complete and expand the hybird computer simulation mentioned in Chapter I.

Gust inputs are not considered in this study but their effect becomes significant at low speeds and therefore should be considered in the next phases of the project.

It is not necessary that the plant and model be of the same order as is the case in this work. It would be worthwhile to implement the model-following scheme of Chapter III for a second order model. In this case two of the plant state variables will have to be chosen as the dominant pair, in determining flying quality. The H matrix of Equation (3.3) would then be changed to reflect this decision.

At present, in order to implement the digital controller the gain matrix K (which includes both the feedforward and feedback gains) must be precalculated off line for the various linearized regions of the flight regime. A study relating the changes in K to the changes in the plant system matrix over these linearized regions would be very beneficial especially if a functional relationship could be derived.

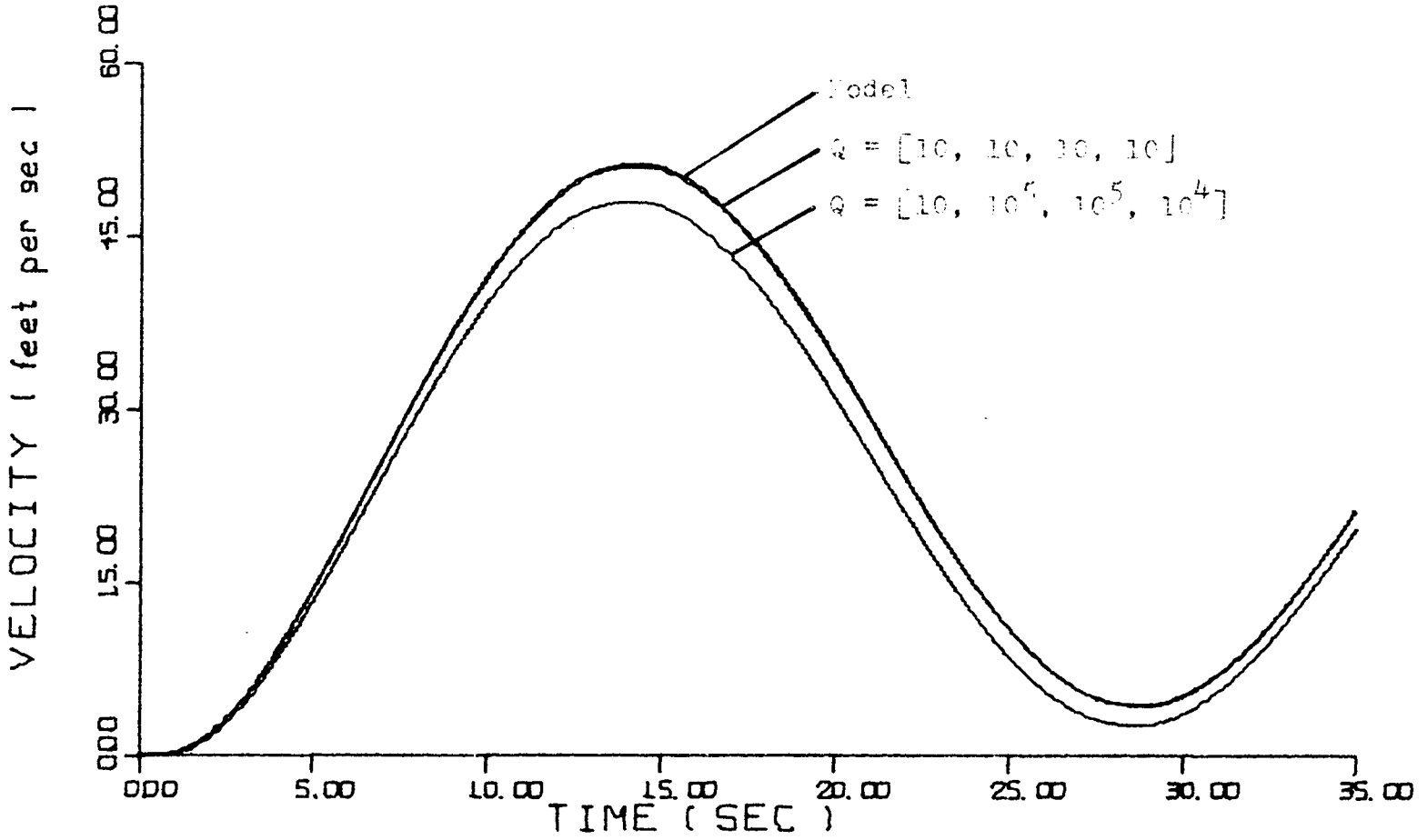

Figure 4.1. Velocity Response for Case I

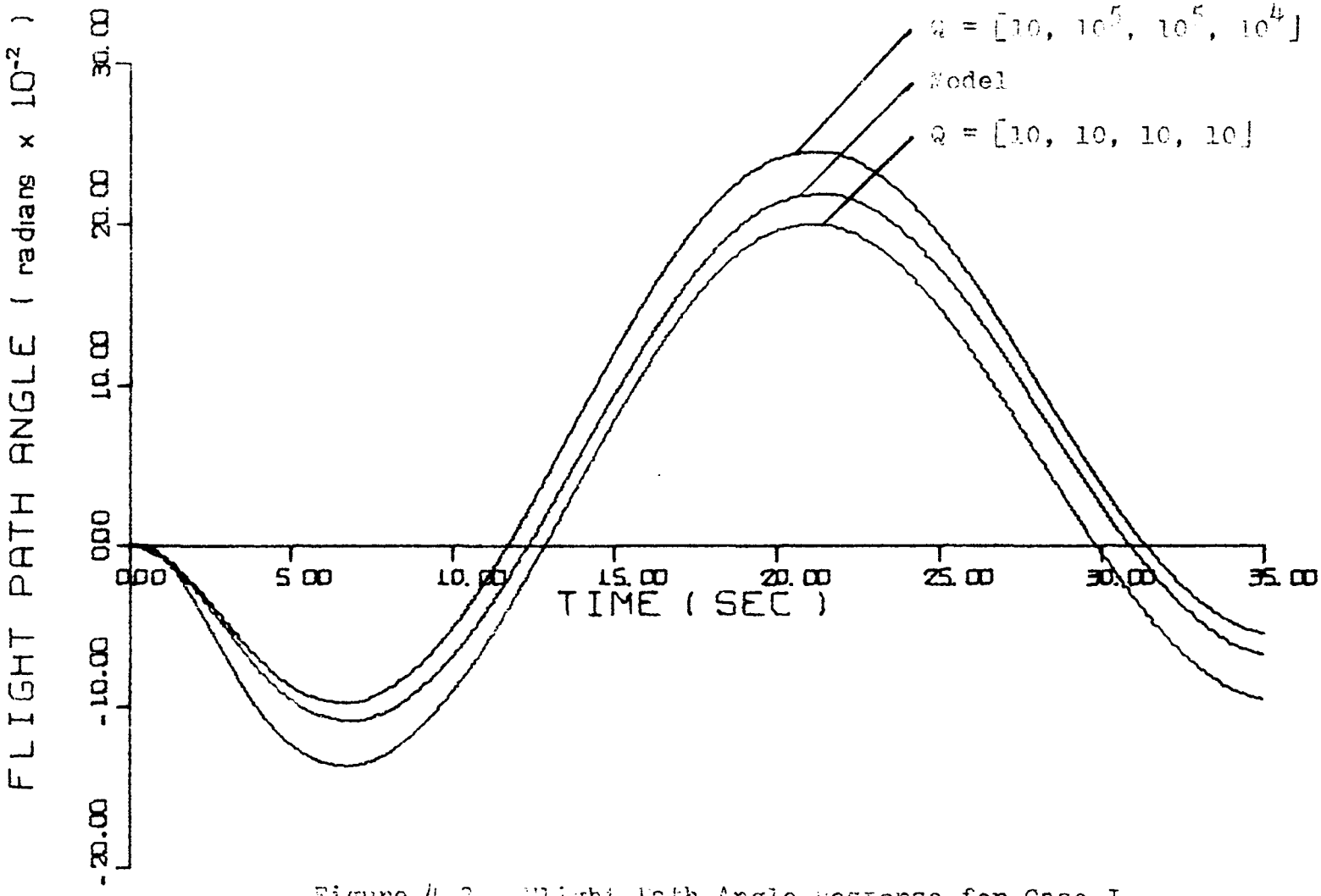

Figure 4.2. Flight Path Angle Response for Case I

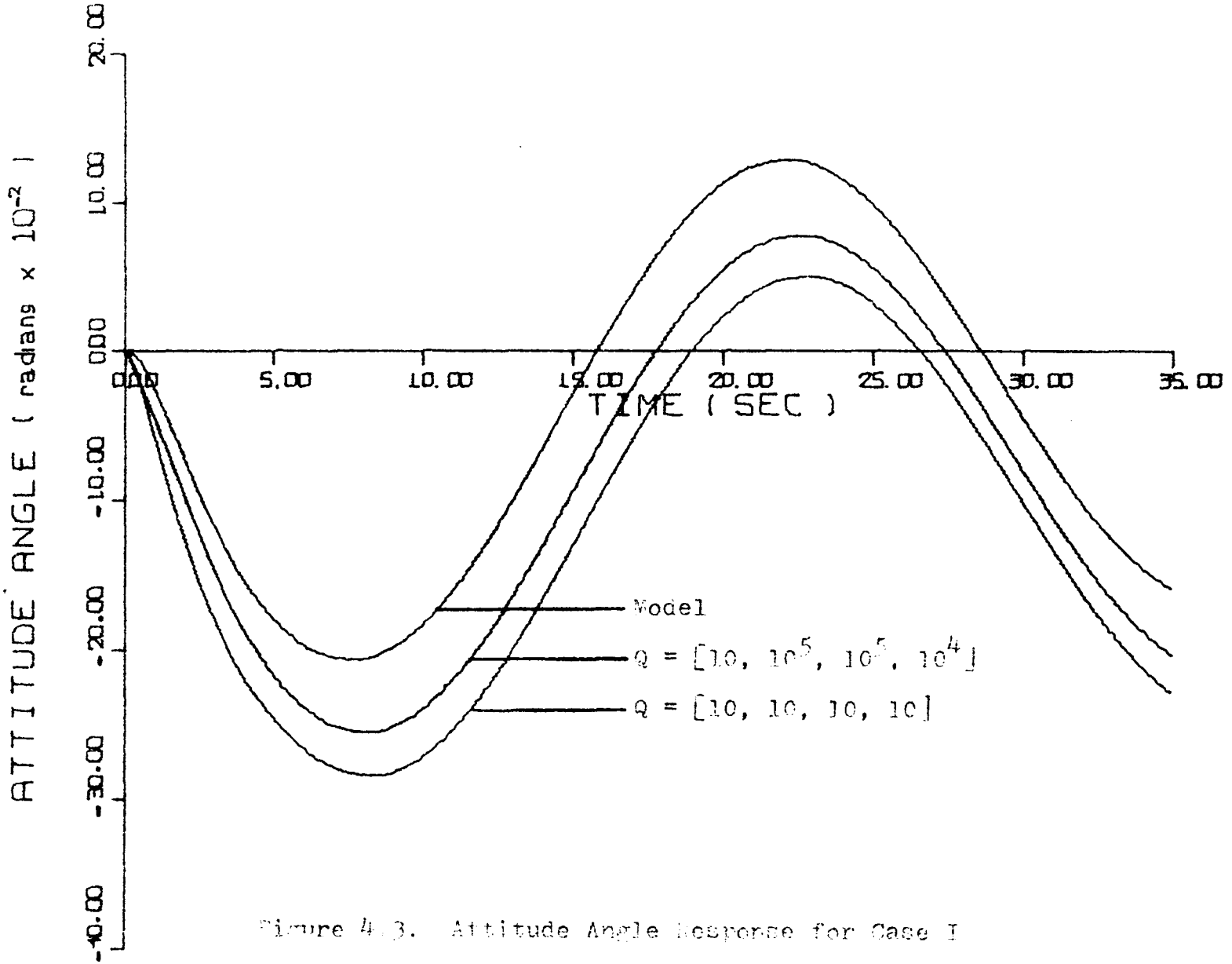

Figure 4.3. Attitude Angle Response for Case I

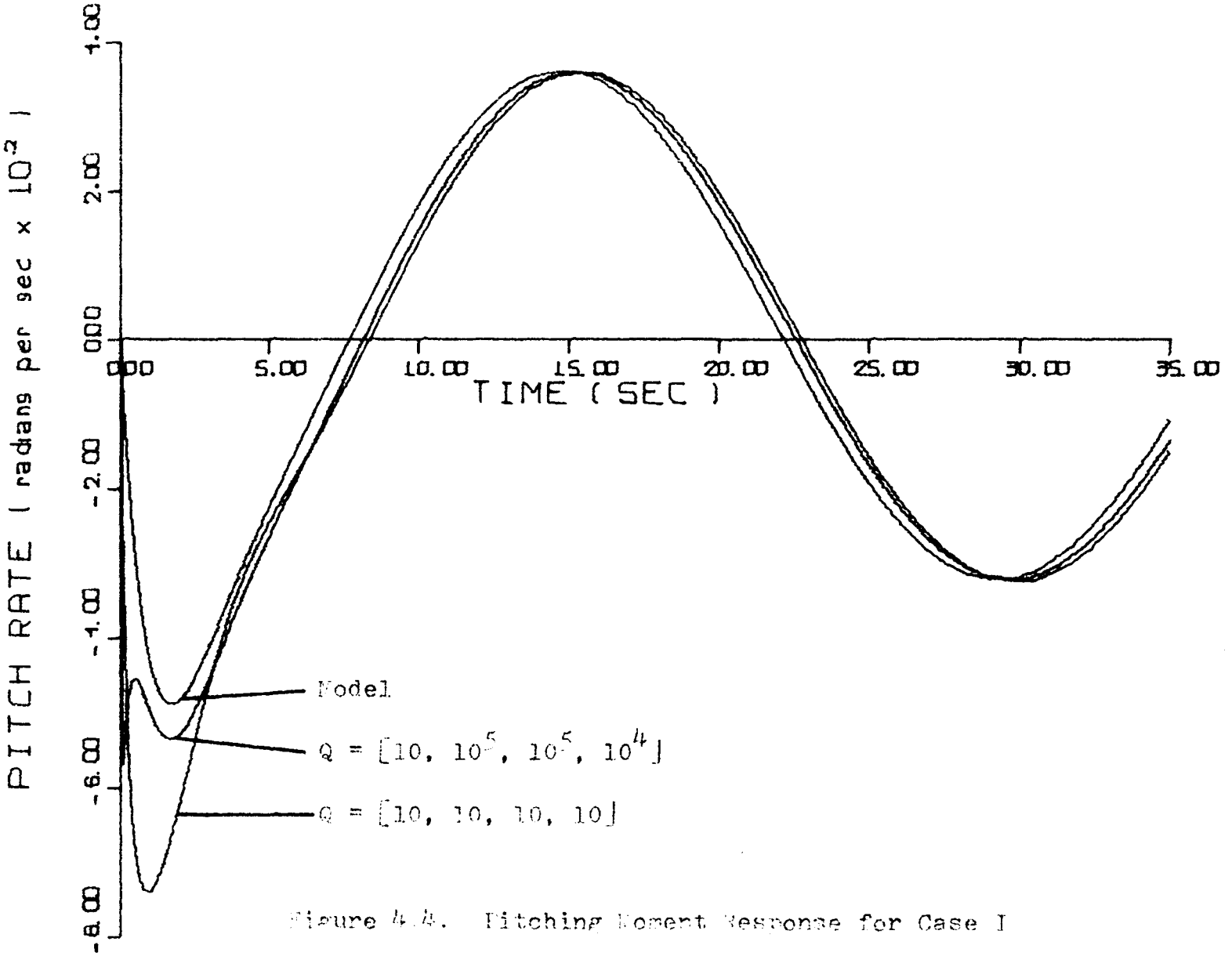

Figure 4.4. Pitching Moment Response for Case I

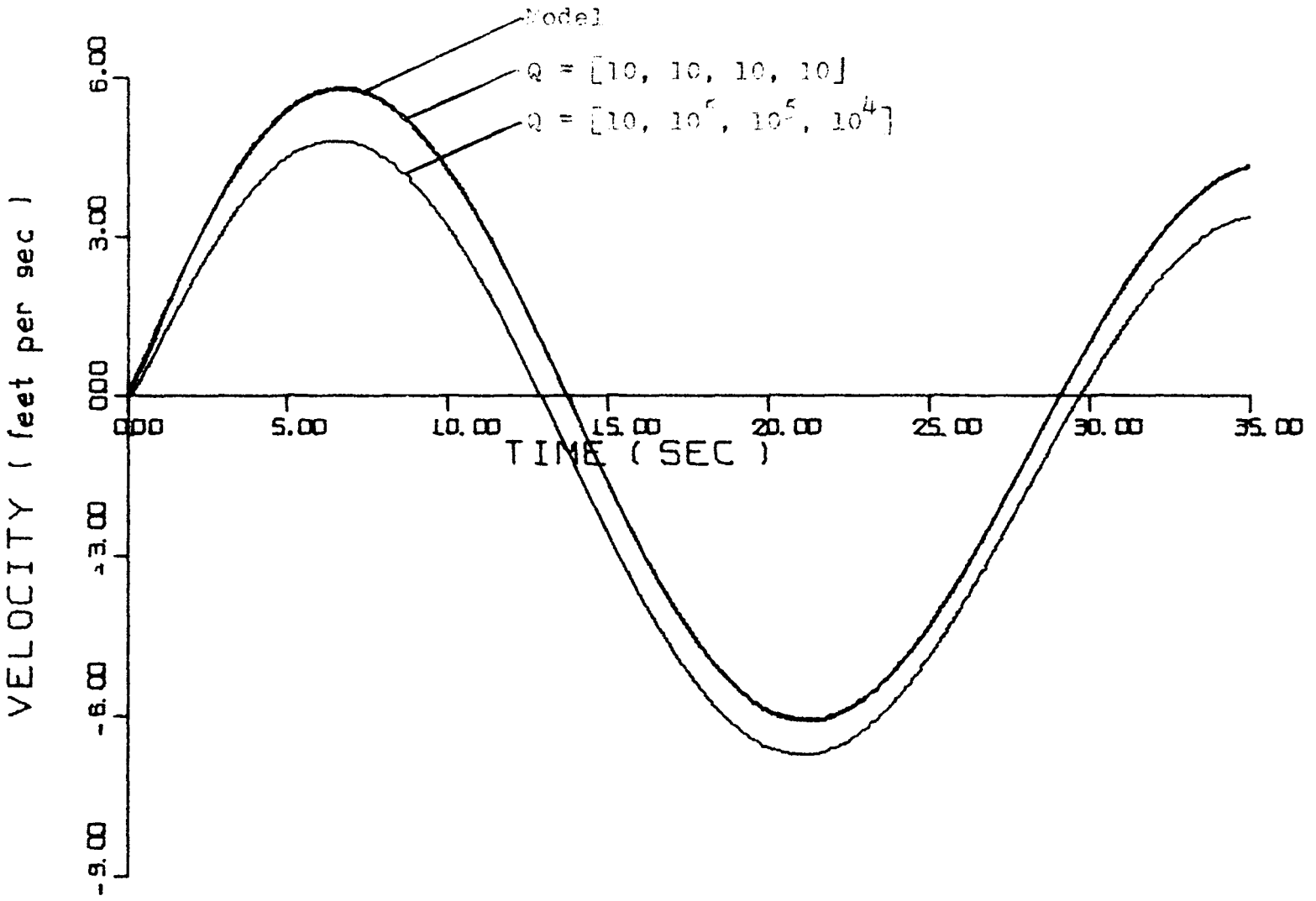

Figure 4.5. Velocity Response for Case II

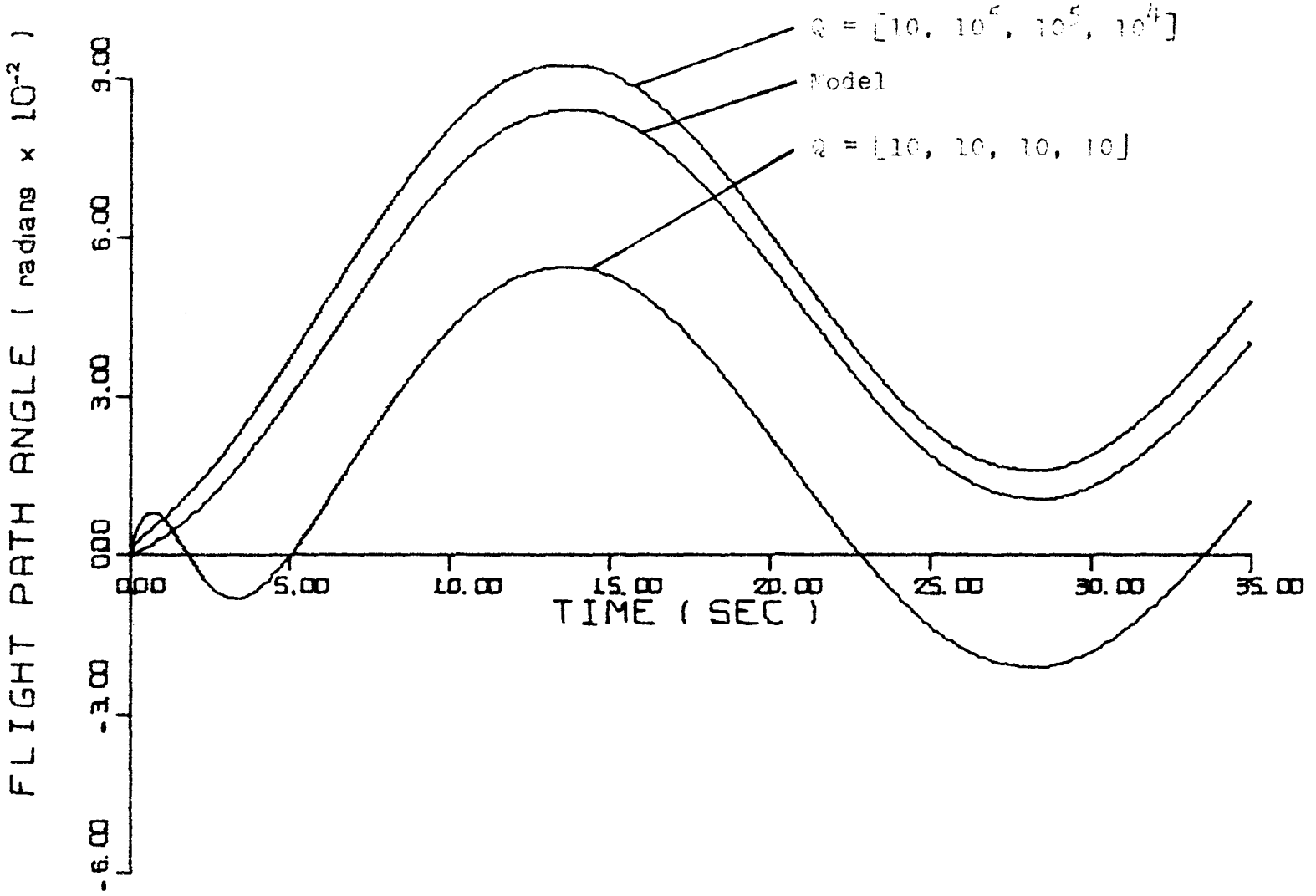

Figure 4.6. Flight Path Angle Response for Case II

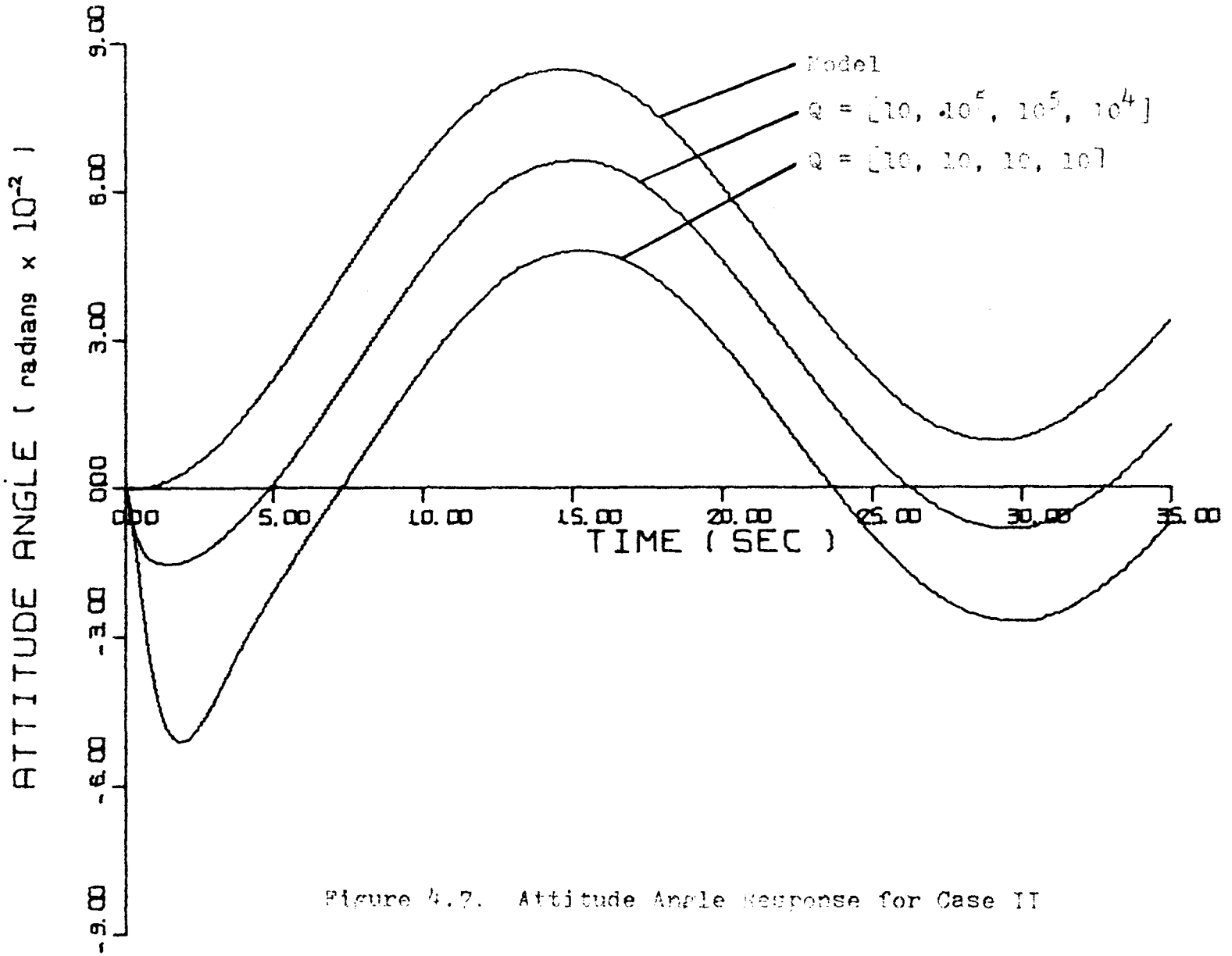

Figure 4.2. Attitude Angle Response for Case II

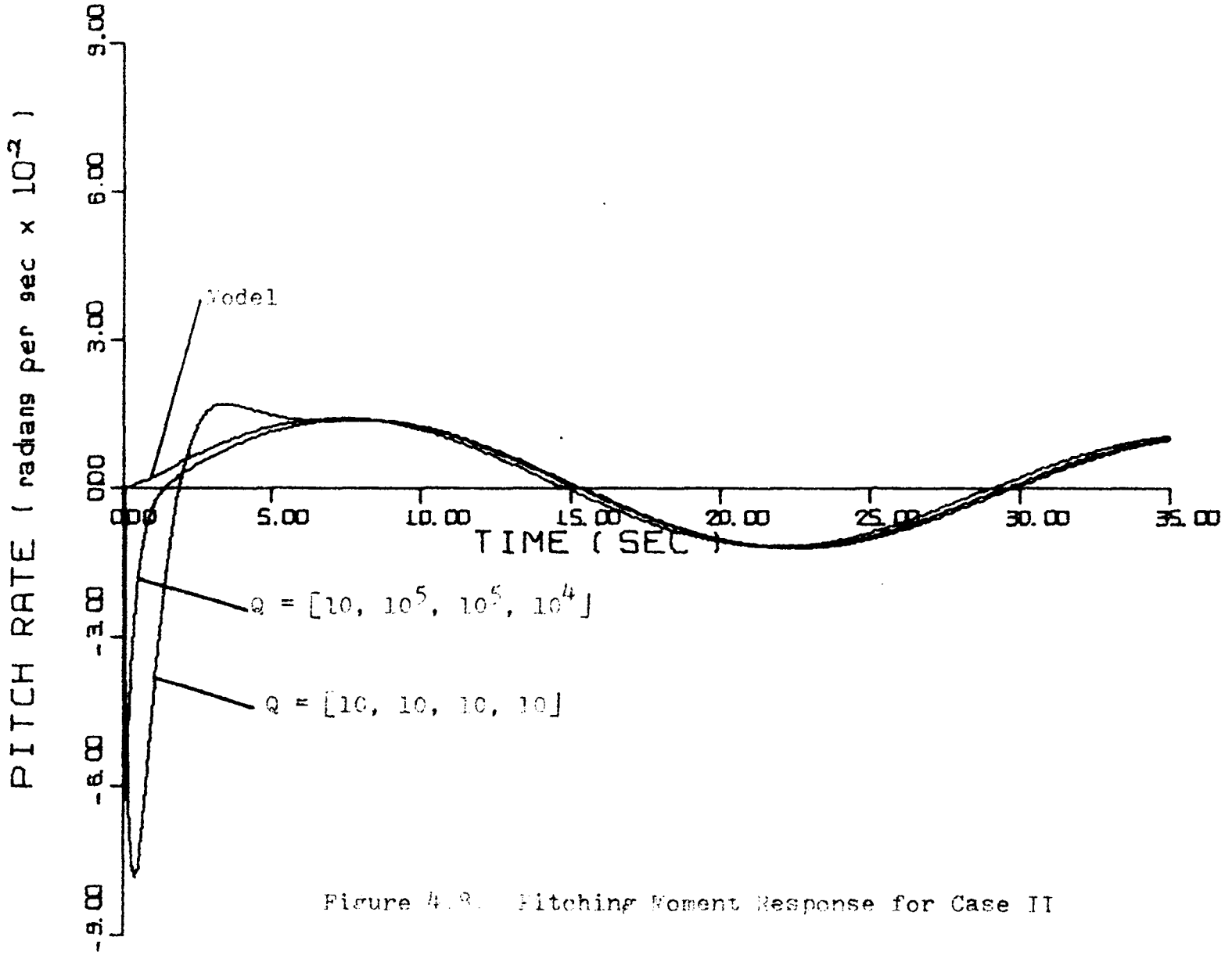

Figure 4.8 Pitching Moment Response for Case II

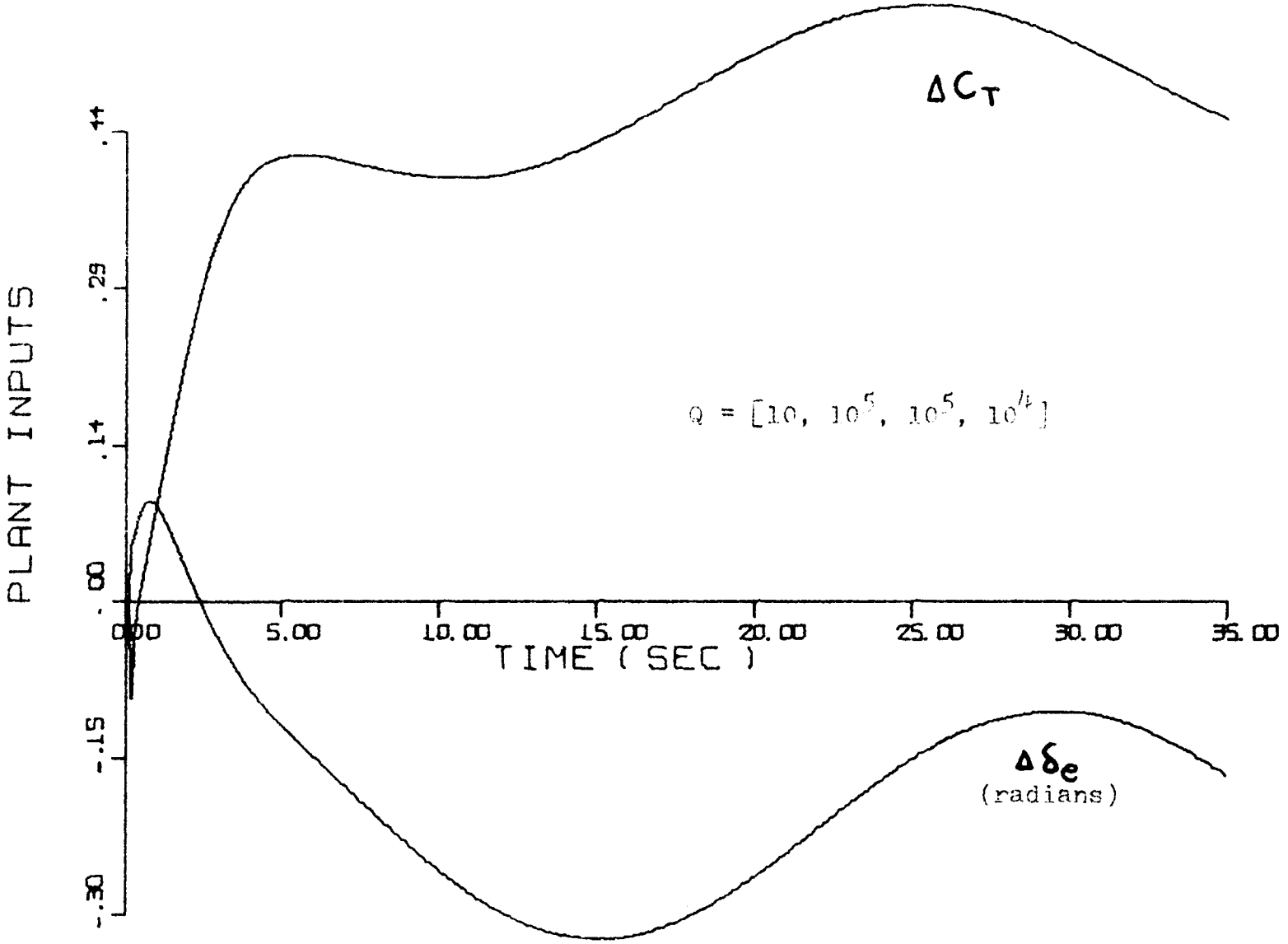

Figure 4.9. Plant Input Signals for Case I

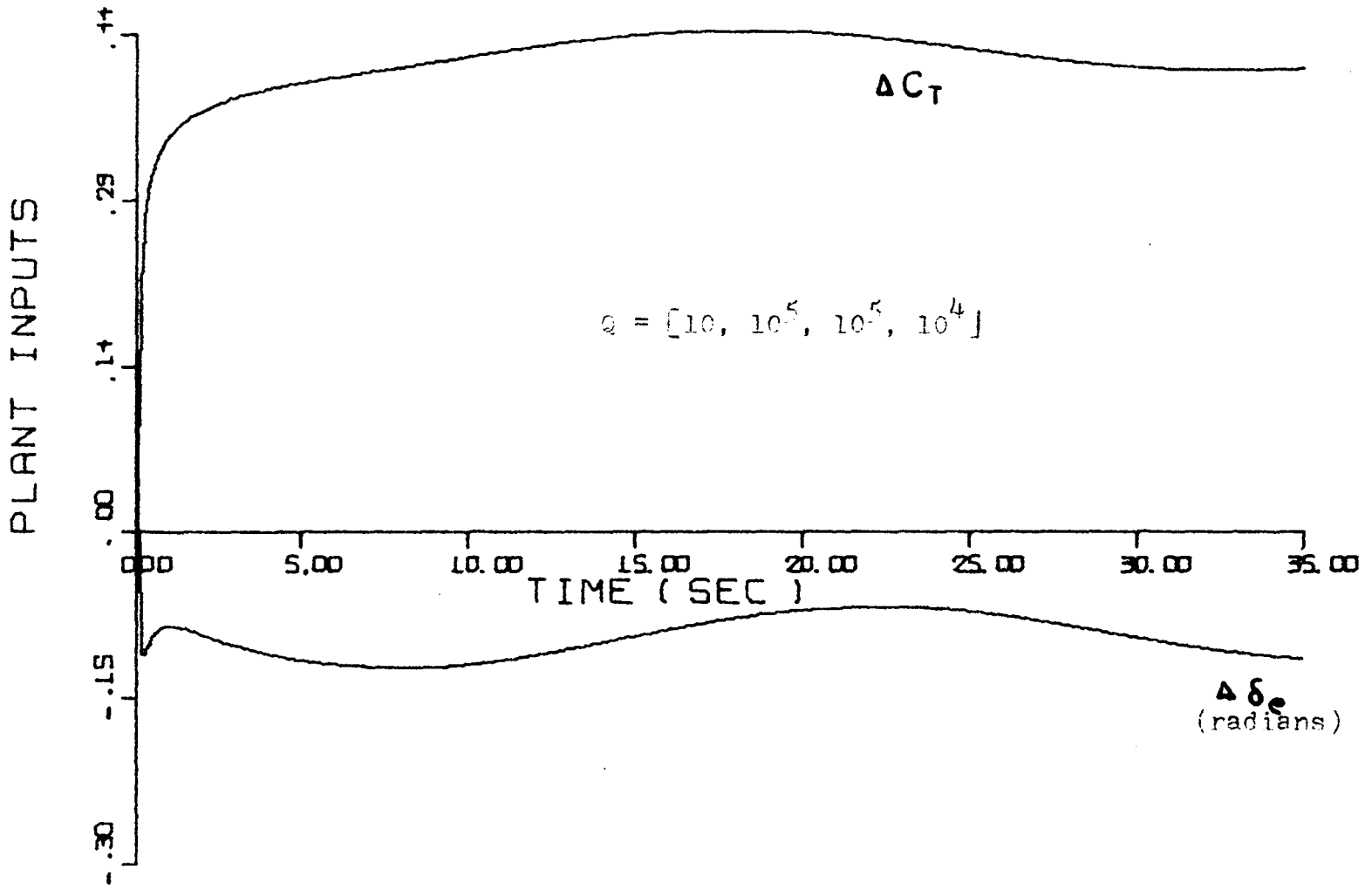

Figure 4.10. Plant Input Signals for Case II

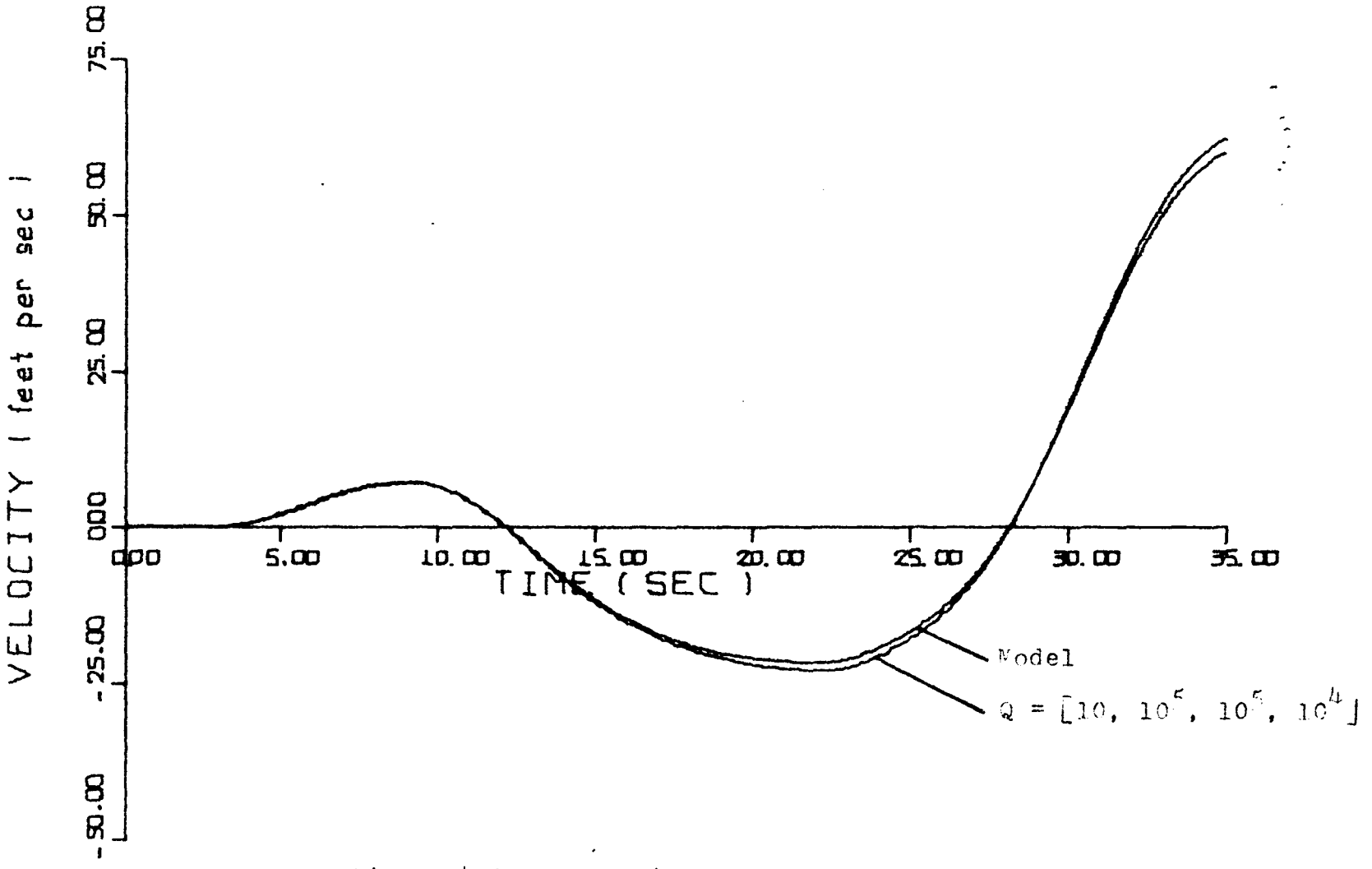

Figure 4.11. Velocity Response for Case III

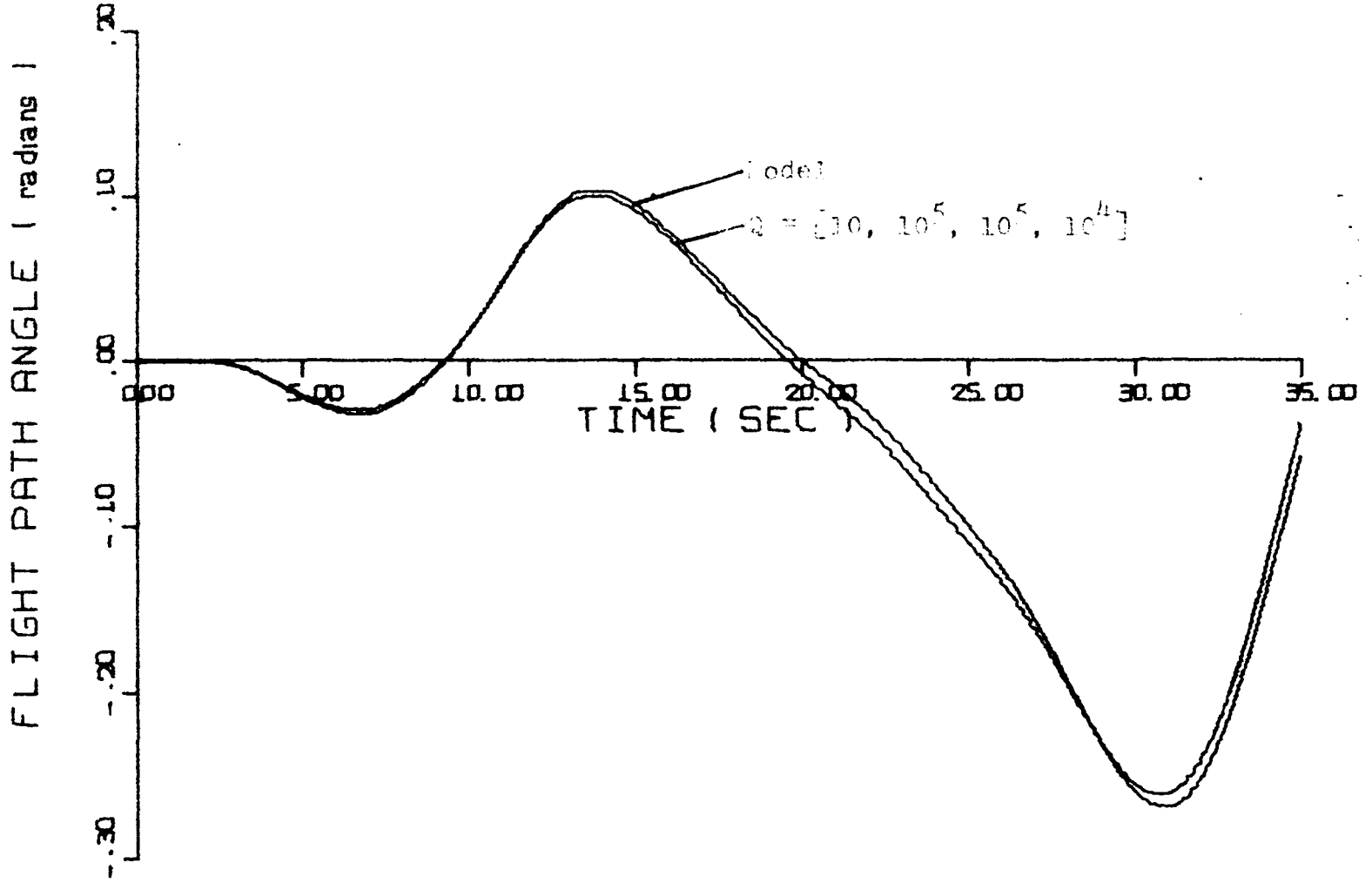

Figure 4.12. Flight Path Angle Response for Case III

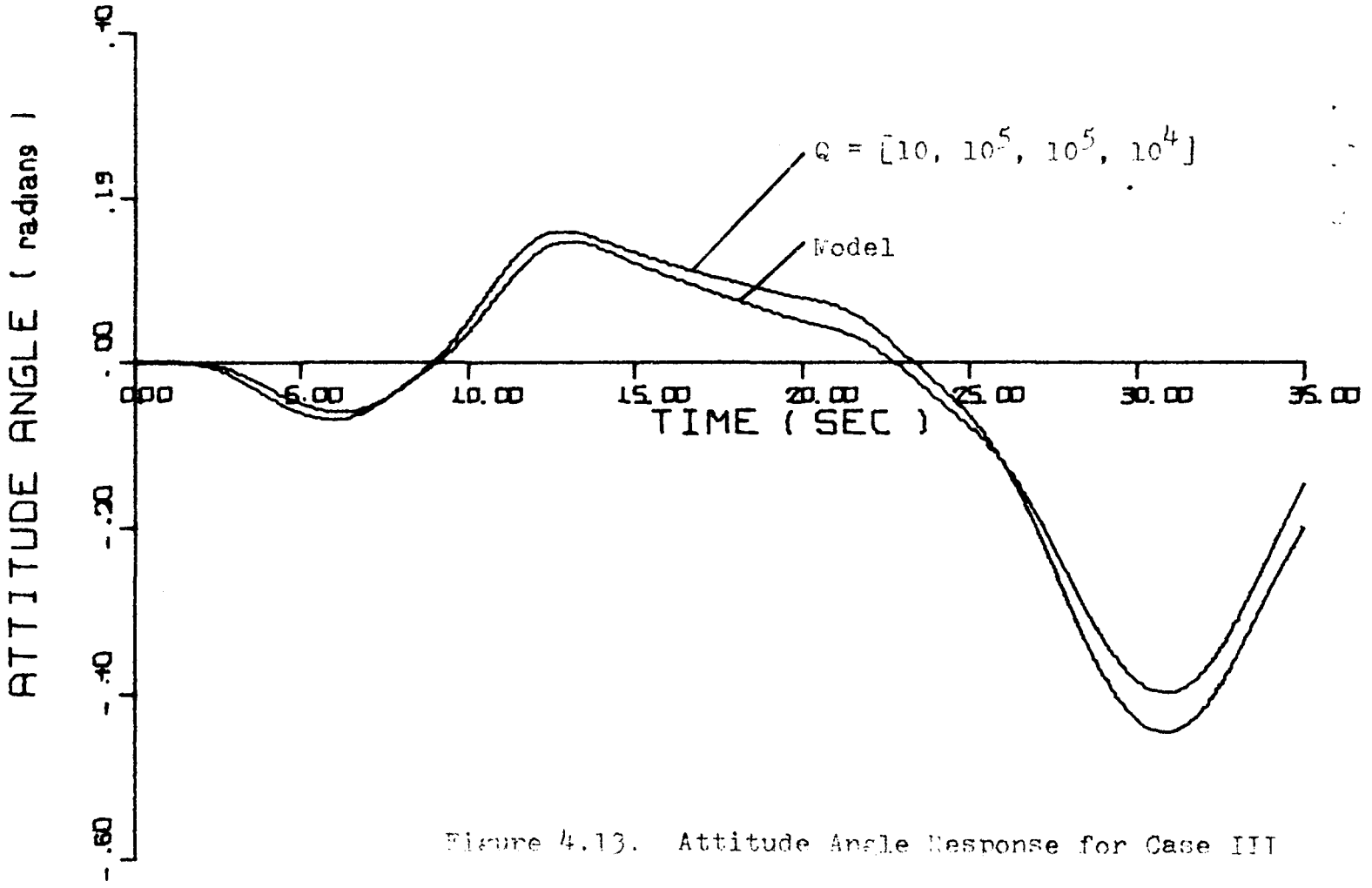

Figure 4.13. Attitude Angle Response for Case III

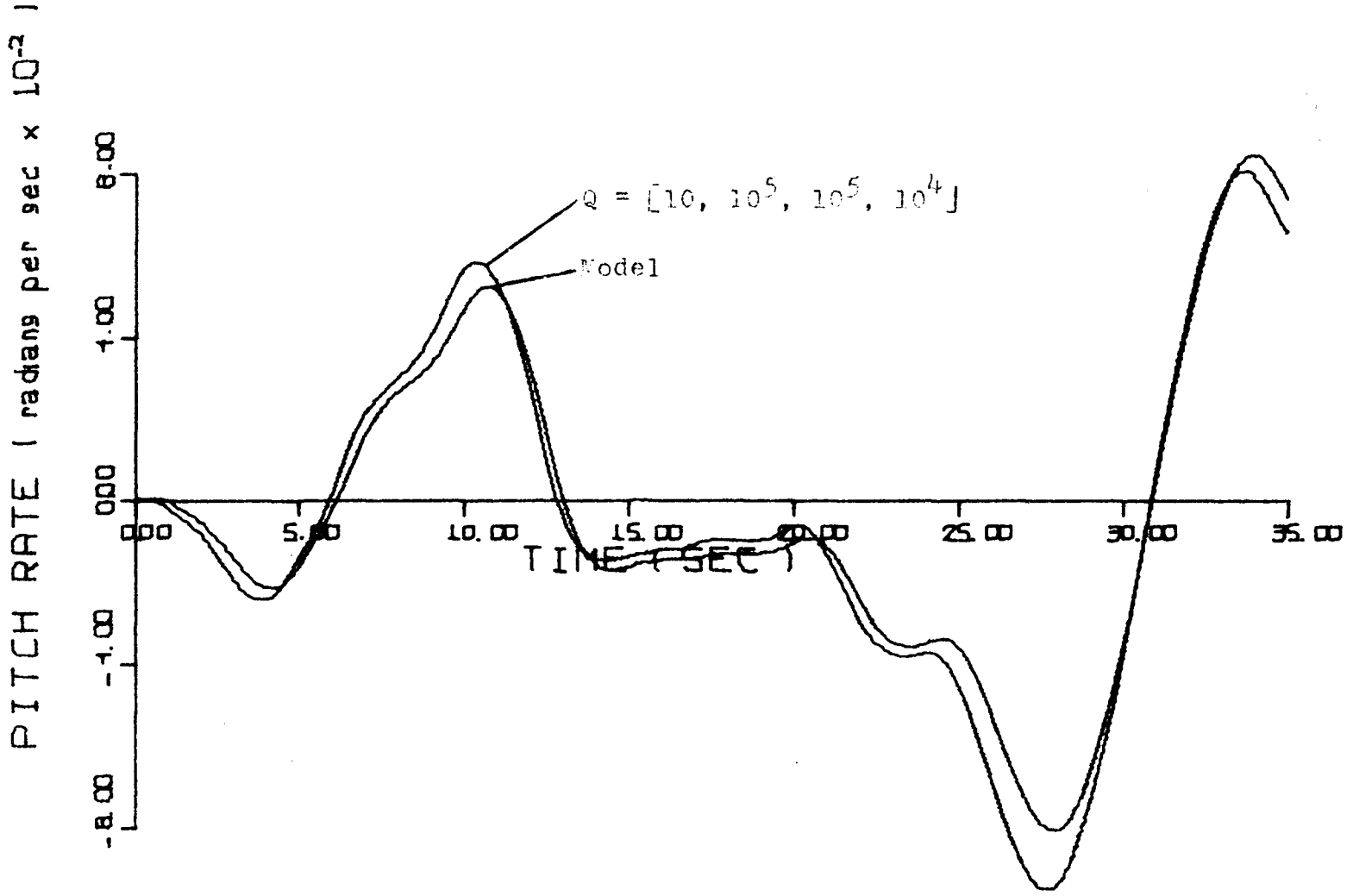

Figure 4.14. Pitching Moment Response for Case III

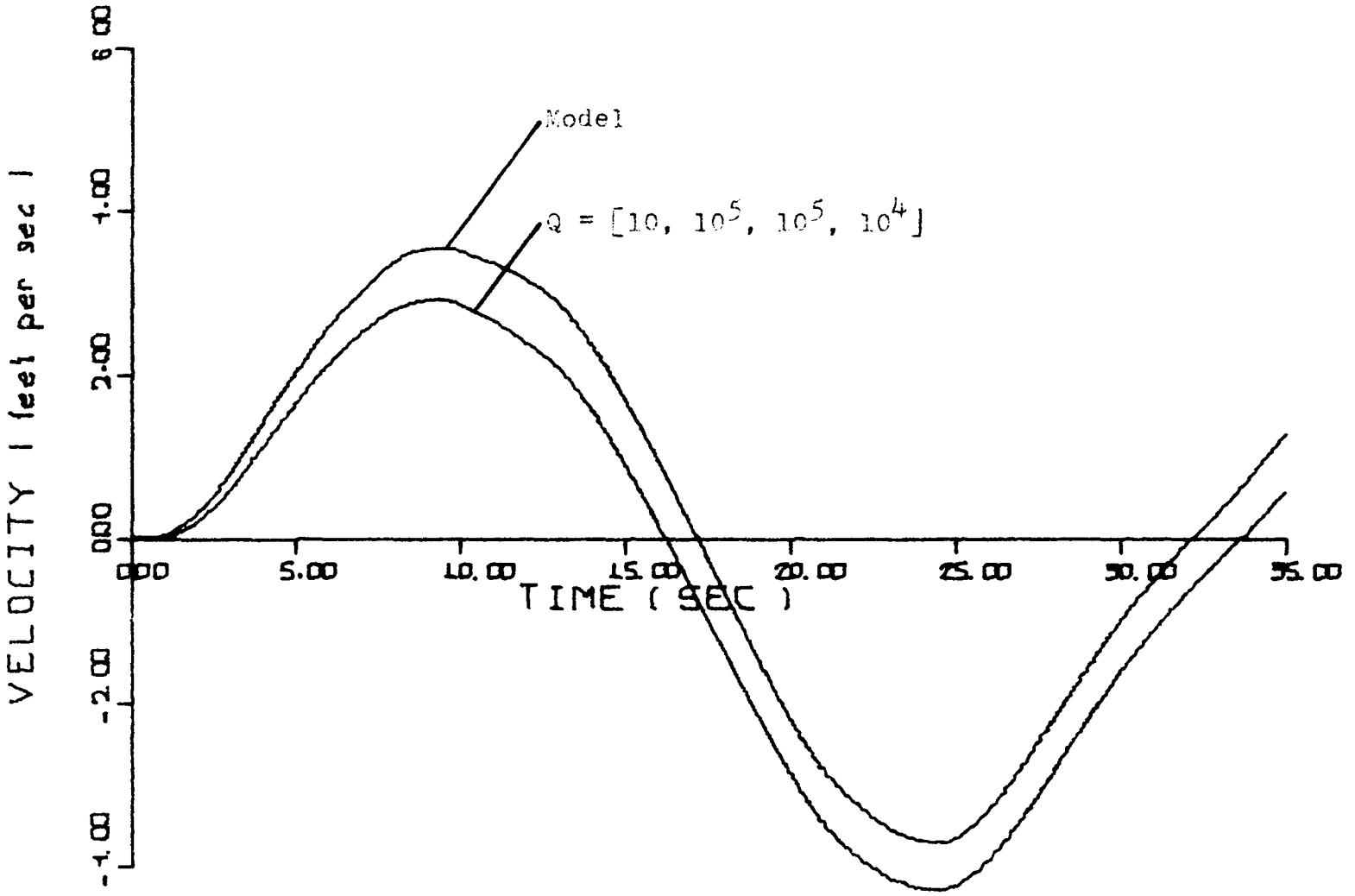

Figure 4.19 Velocity Response for Case IV

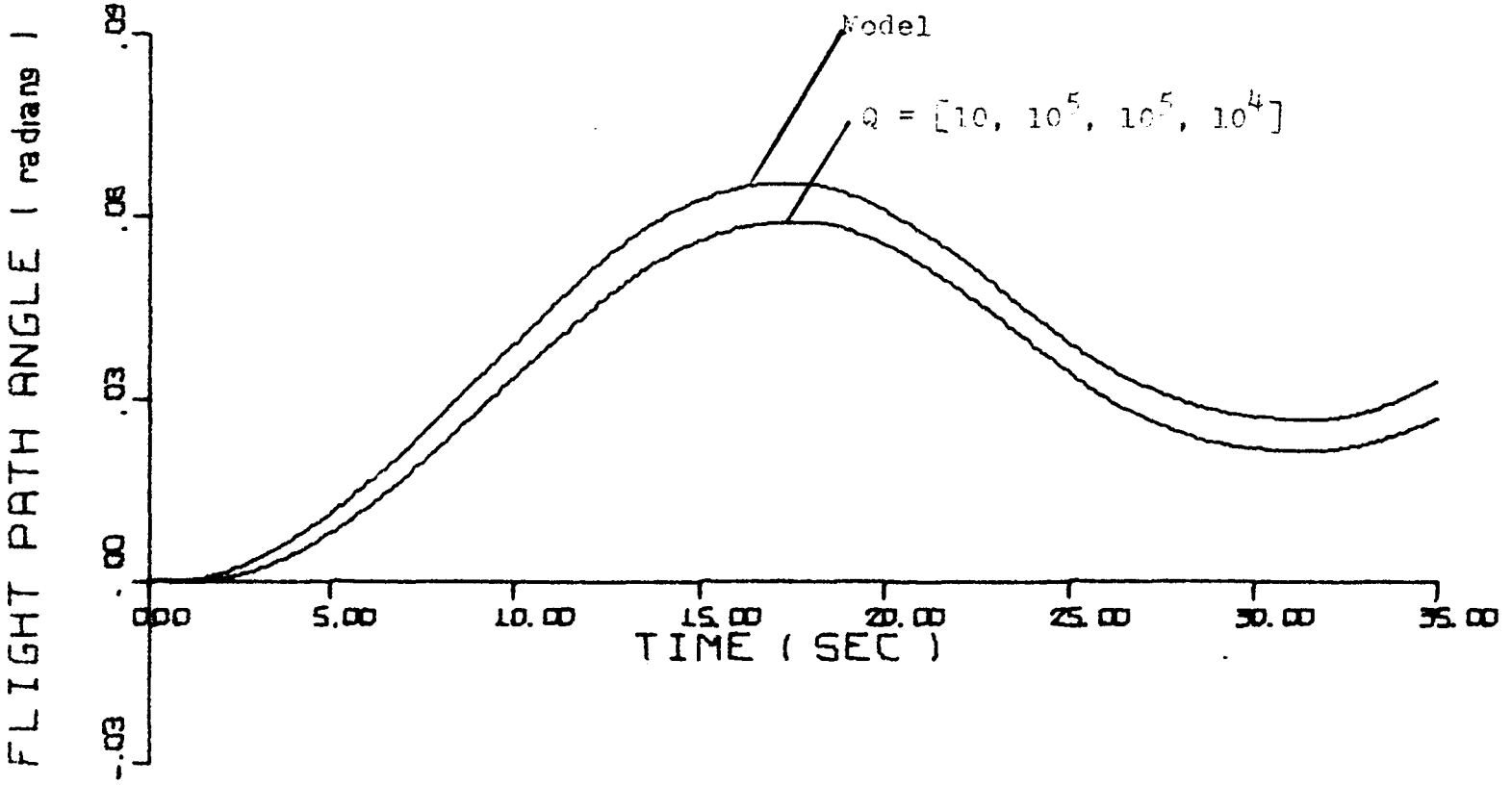

Figure 4.16. Flight Path Angle Response for Case IV

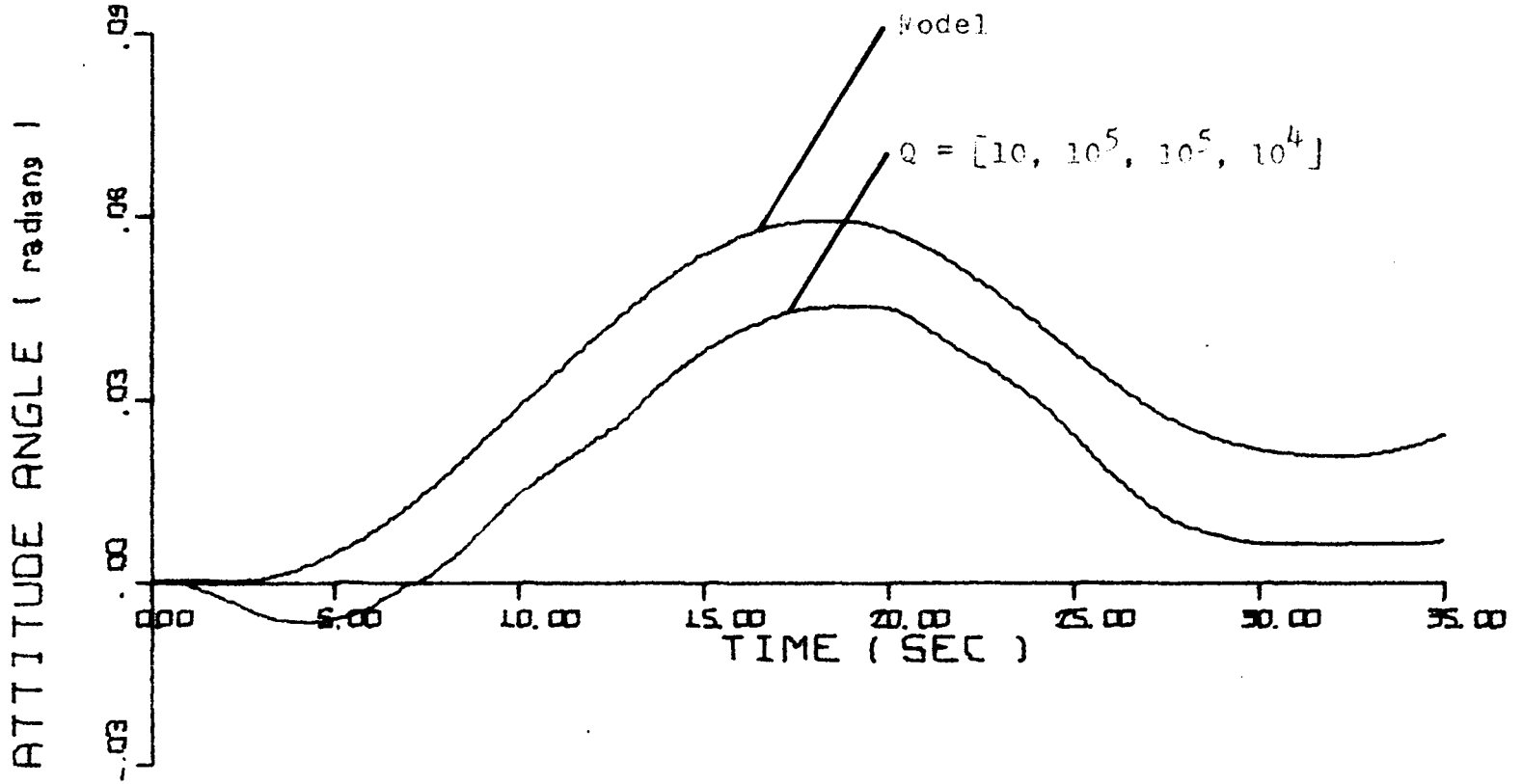

Figure 4.12. Attitude Angle Response for Case IV

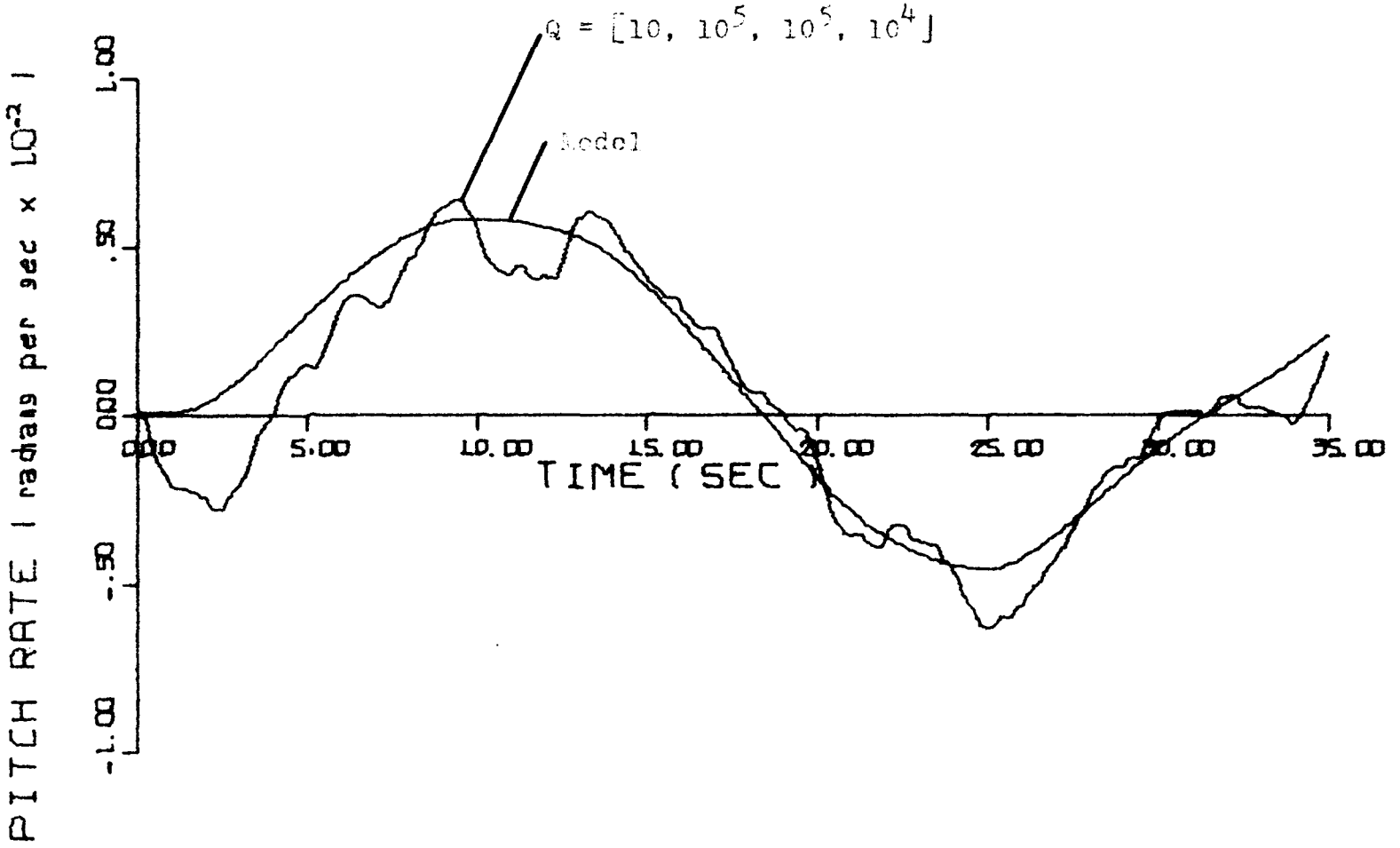

Figure 4.18. Pitching Moment Response for Case IV

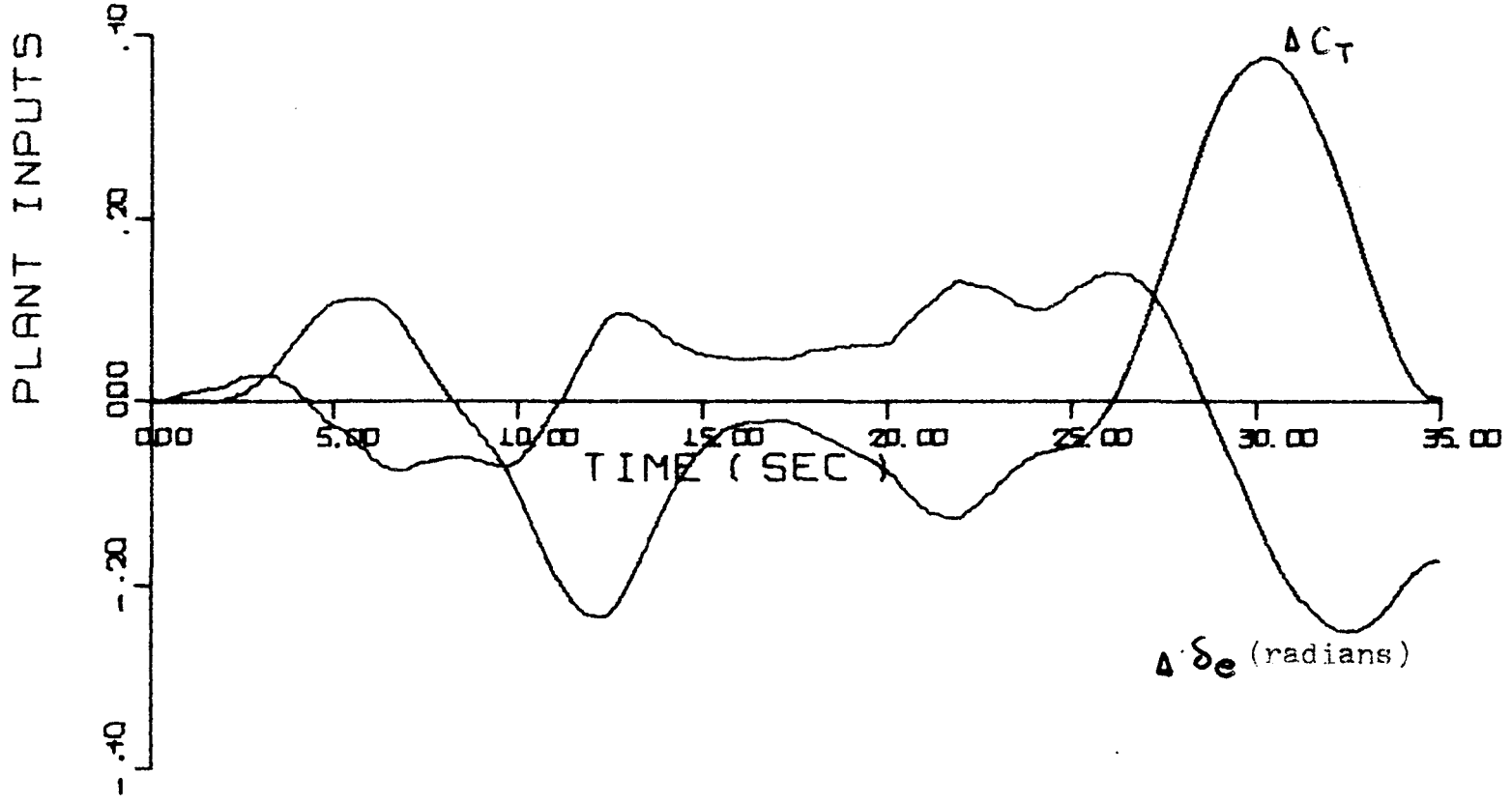

Figure 4.10. Plant Input Signals for Case III

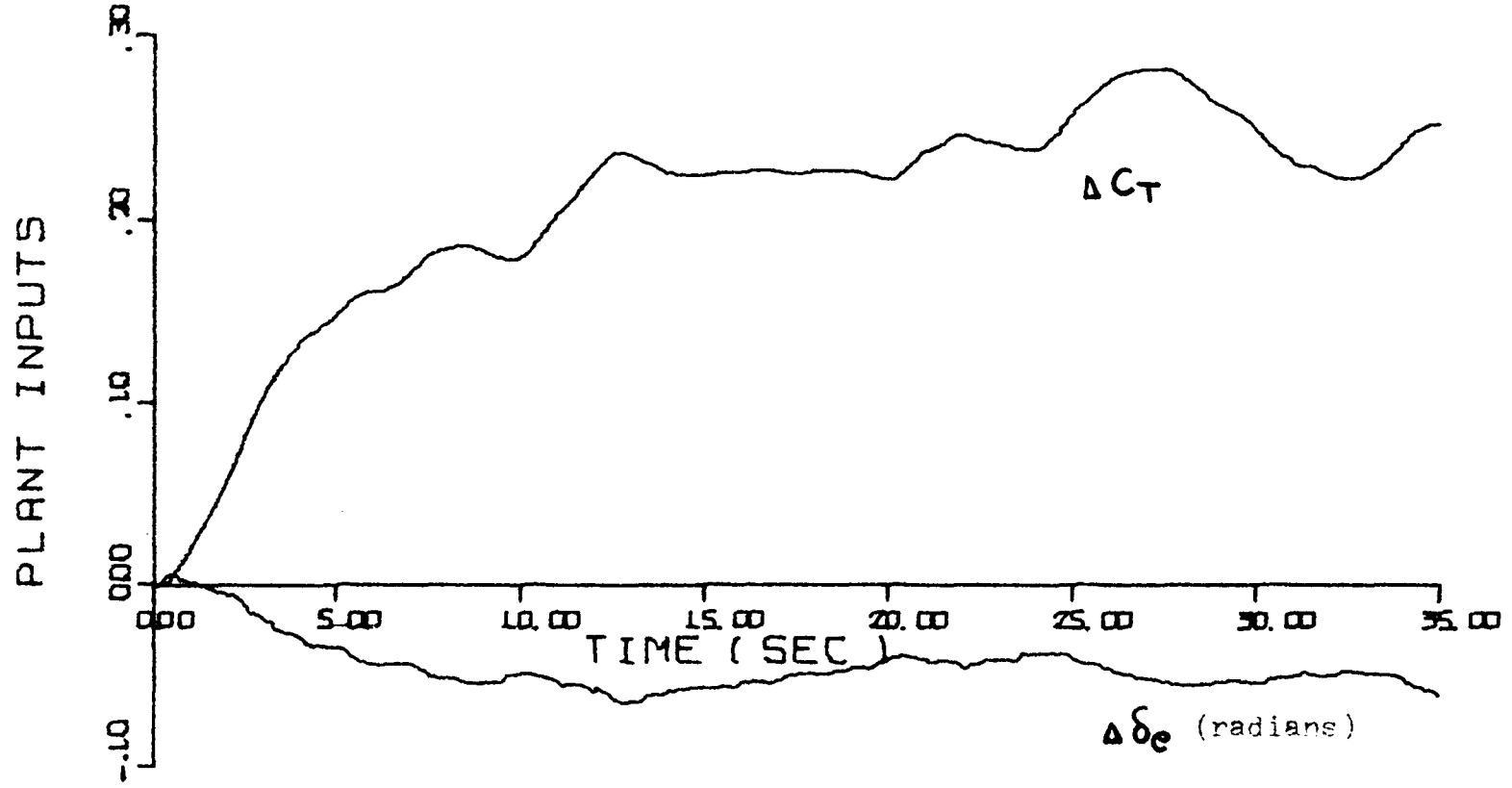

Figure 4.20. Plant Input Signals for Case IV

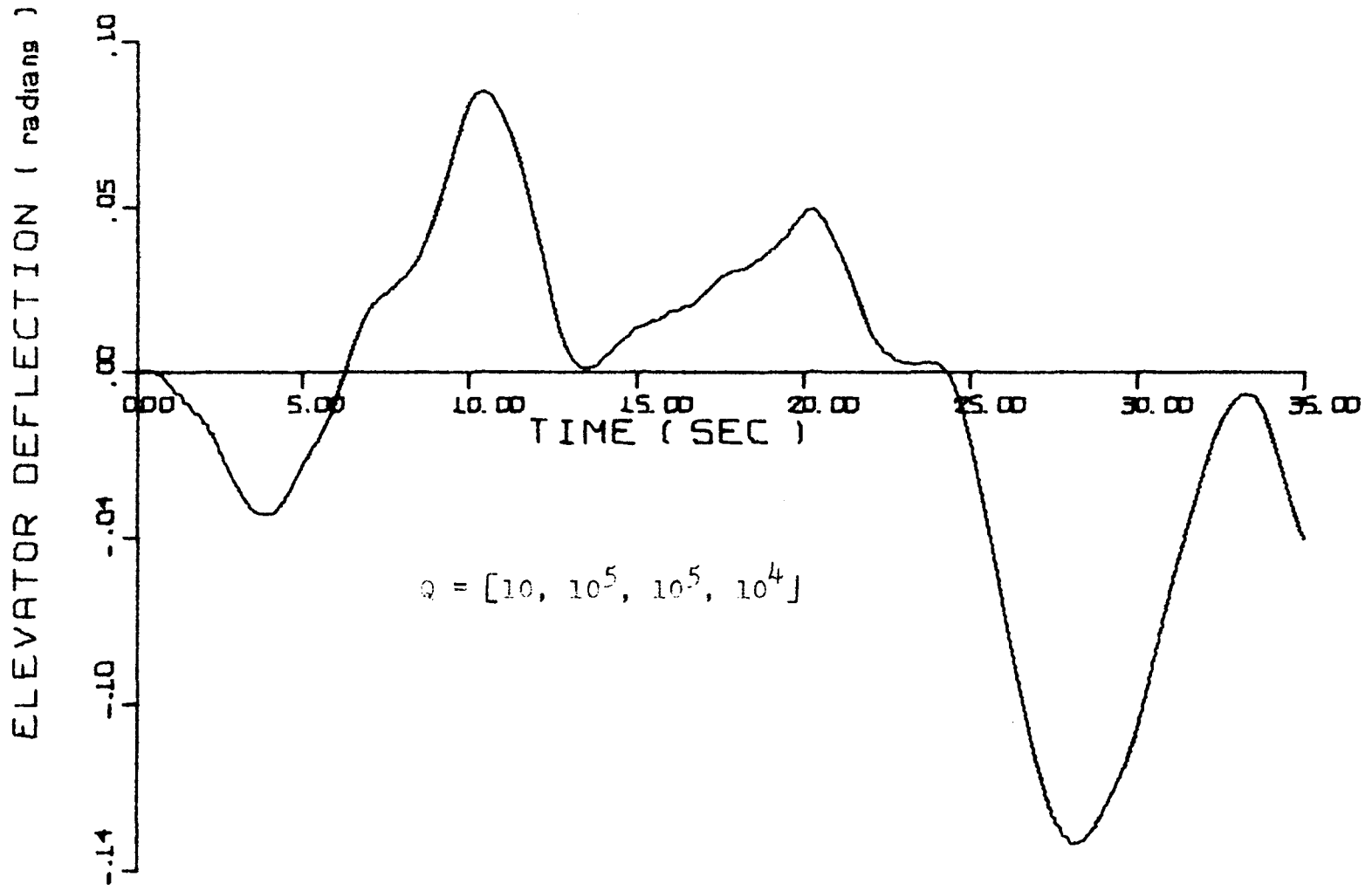

Figure 4.21. Pilot Command Signal for Case III

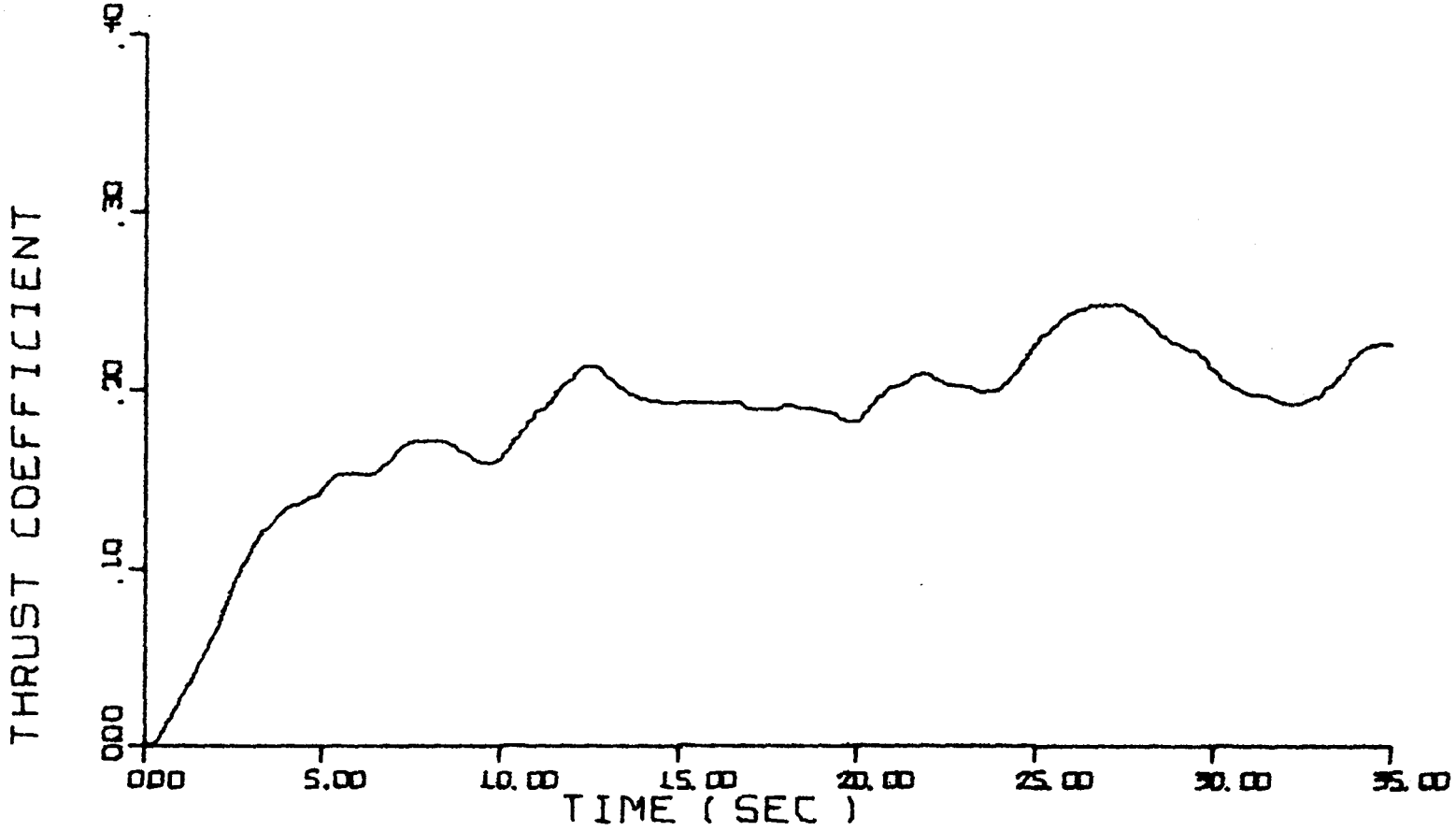

Figure 4.22 Pilot Command Signal for Case IV

BIBLIOGRAPHY

Literature Cited

1. Ogata, Katsuhiko. State Space Analysis of Control Systems. Englewood Cliffs, New Jersey: Prentice-Hall, 1967.
2. Kirk, D. E. Optimal Control Theory: An Introduction. Englewood Cliffs, New Jersey: Prentice-Hall, 1970.
3. Etkin, Bernard. Dynamics of Atmospheric Flight. New York: John Wiley & Sons, 1972.
4. Discussion with Dr. F. H. Lutze, Jr., Associate Professor of Aerospace Engineering, Virginia Polytechnic Institute and State University, Blacksburg, Virginia.
5. Tyler, J. S., Jr. "The Characteristics of Model-Following Systems as Synthesized by Optimal Control." IEEE Transactions on Automatic Control, Vol. AC-9, October 1964.
6. Erzberger, Heinz. On the Use of Algebraic Methods in the Analysis and Design of Model-Following Control Systems. NASA: TN D-4663, July 1968.
7. Sage, A. P. Optimum Systems Control. Englewood Cliffs, New Jersey: Prentice-Hall, 1968.
8. Personal communication with Dr. R. C. Montgomery, Flight Dynamics and Control Division, NASA-Langley Research Center, Hampton, Virginia.

APPENDIX A

LINEARIZATION OF THE AERODYNAMIC DATA

The flight regime is determined by the range of the thrust coefficient and angle of attack. In this study the ranges considered are

α = (-5 to 10) degrees

C_T = (0.0 to 3.5).

As shown in Figures A.1 and A.2, the available aerodynamic data is a function of these two variables for a given flap deflection. These figures are only a partial representation of the entire data. This data was obtained from wind tunnel tests on a model of the EBF-STOL class of aircraft [8]. It is nonlinear and is therefore approximated by straight line segments over the flight regime being considered. To facilitate this approximation the ranges on α and C_T are represented by the discrete values

α = (-5, 0, 5, 10) degrees

C_T = (0.0, 0.5, 1.0, 1.5, 2.0, 2.5, 3.0, 3.5).

Due to the non-linearity and parametric form of the data, an attempt to find analytic expressions for the force coefficients as functions of α and C_T was not made. Instead, the stability derivatives are held constant over piecewise linear portions of the

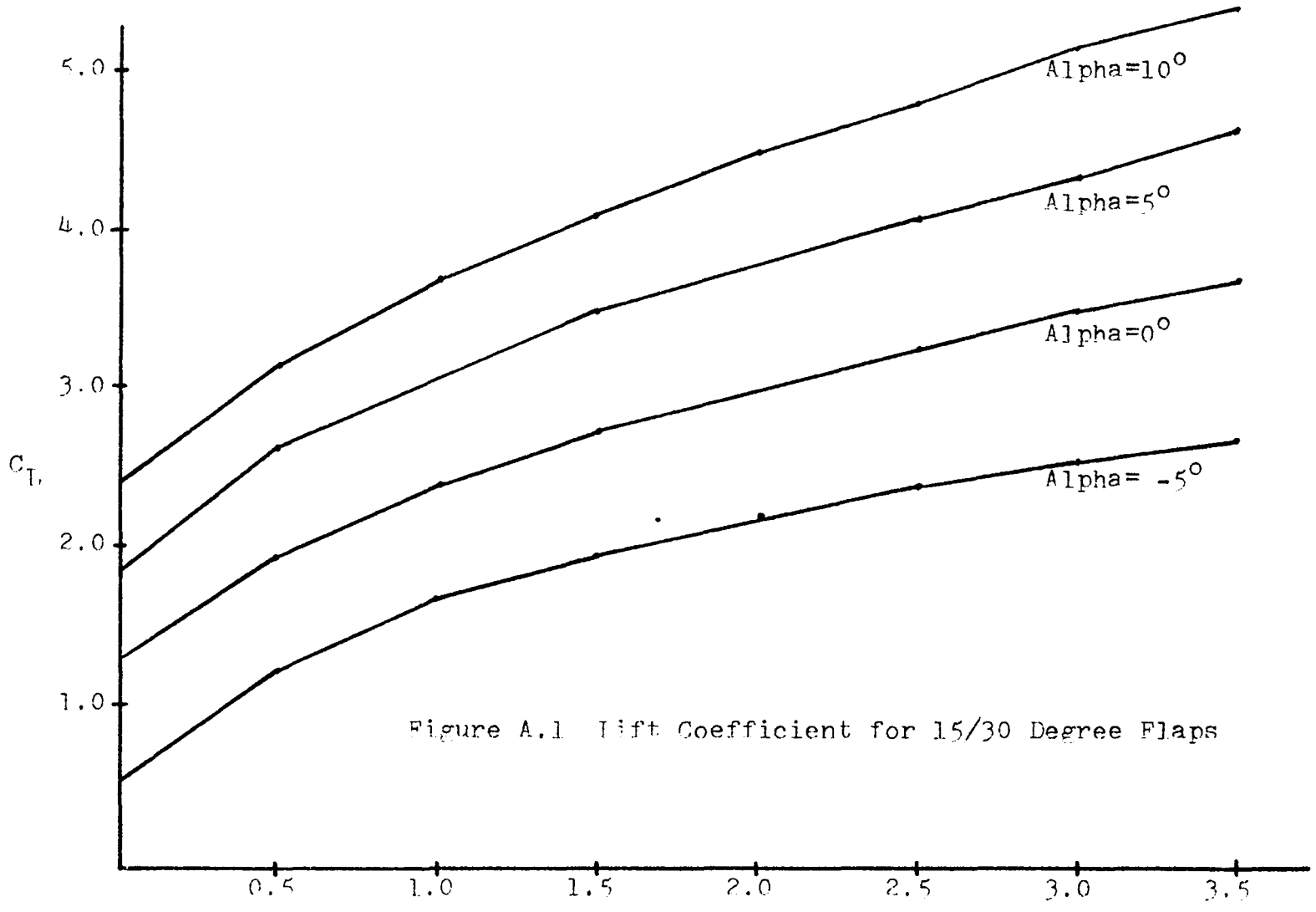

Figure A.1 Lift Coefficient for 15/30 Degree Flaps

Figure A.2 Moment Coefficient for Zero Degree Flaps

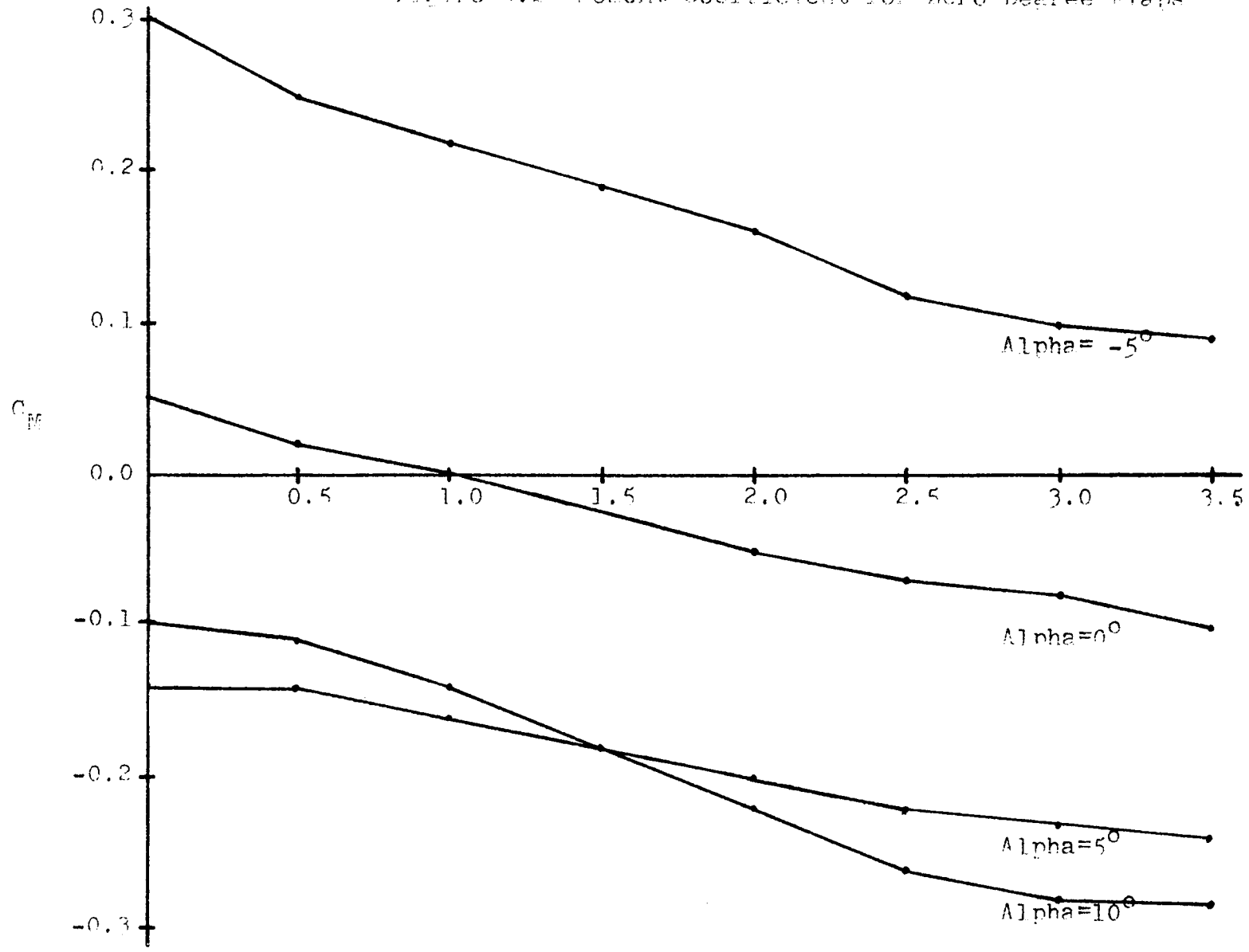

flight regime, which can be conveniently linearized by considering 5^{o} increments in alpha and half unit increments in the thrust coefficient. The nominal values are then taken as the center of the resulting parallellogram, over which the stability and control derivatives are constant.

This thesis only considers control of the aircraft about a linearized point of the flight regime in order to demonstrate the technique. Normally, in a digital simulation new system and control matrices and gains are calculated for each linearized portion of the flight regime. In a real-time hybrid simulation, such as that discussed in the Introduction, these matrices and gains would be precalculated and stored in memory. The analog section could then determine when alpha or the thrust coefficient have exceeded the present linear portion and update the system with new values. Of course, this step can also be performed at regular intervals as part of the cycling time.

A.1 Stability and Control Derivatives

Stability derivatives are related to partial derivatives of the force and moment coefficients with respect to the state variables while control derivatives are related to partial derivatives of these coefficients with respect to the control variables. The derivatives needed for this study are

$$C_{L_\alpha} \qquad C_{D_\alpha} \qquad C_{M_\alpha}$$

$$C_{L_T} \qquad C_{D_T} \qquad C_{M_T}$$

$C_{L_{\delta_e}}$ $C_{D_{\delta_e}}$ $C_{M_{\delta_e}}$

and C_{M_q}, which is given as -51.7.

The three stability derivatives are calculated from the slopes of the lift, drag, and moment coefficient data (see Figures A.1 and A.2). The remaining control derivatives were determined from [4]. The derivatives take on different values for different flight conditions. The values used for the derivatives are presented in Table I.

A.2 Aerodynamic Data

The range of the different variables in this study is as follows:

$V = 50 - 200$	feet per second
$\alpha = \pm 0.2$	radians
$\theta = \pm 0.4$	radians
$q = \pm 1.0$	radians per second
$\bar{q} = 0 - 100$	pounds per square feet
$\gamma = \pm 0.2$	radians

In addition there are the following aircraft parameters:

$W = 55,100$	pounds
$\bar{c} = 10.5$	feet
$S = 800$	square feet
$I_y = .248 \times 10^6$	slugs · square feet
$\rho = .238 \times 10^{-2}$	slugs per foot cubed

g = 32.2	feet per second squared
m = 1715	slugs

APPENDIX B

COMPUTER PROGRAM LISTING

```
      COMMON AA(12,12),A(10,10),B(10,2),R(2,2),H(4,10),Q(4,4),
     1 QQ(10,10),HQ(10,4),BT(2,10),BTP(2,10),BTPB(2,2),RB(2,2),
     2 RBT(2,10),ADT2(12,12),FF(2,10),PP(10,10),BFF(10,10),
     3 V(10,10),VT(10,10),L(10),E(10),HT(10,4),FFT(10,2),GG,
     4 VTP(10,10),VTPV(10,10),FTR(10,2),EADT2(12,12),FRF(10,10),
     5 TT(2,10),ST(10),X(10),T(10),S(10),U(2),EADT(12,12),
     6 S1(12,12),S2(12,12),N,NN,M,KN,DT,NNM,MM,N2,K1,K2,KK,EE,G,
     7  YY(8,100),Y(2,100),XV(350)
C
      INTEGER E,GG,G,EE
      KN=2000
      NN=10
      M=2
      DT=.1
      KK=4
      N=NN+M
      K1=KK*KK
      K2=KK*NN
      NNM=NN*M
      MM=M*M
      N2=NN*NN
      READ(5,8)  ((AA(I,J),J=1,N),I=1,N)
      READ(5,1)  ((H(I,J),J=1,NN),I=1,KK)
      READ(5,1)  ((R(I,J),J=1,M),I=1,M)
      WRITE(6,10)
      WRITE(6,2) ((AA(I,J),J=1,N),I=1,N)
      WRITE(6,11)
      WRITE(6,9) ((H(I,J),J=1,NN),I=1,KK)
      WRITE(6,11)
      WRITE(6,3) ((R(I,J),J=1,M),I=1,M)
    4 READ(5,1)  ((Q(I,J),J=1,KK),I=1,KK)
      DO 5 I=1,NN
```

```
  5    X(I)=0.0
       X(10)=-5.
       WRITE(6,10)
 1     FORMAT(7F10.5)
 2     FORMAT(2X,12F10.6)
 3     FORMAT(2X,2F10.5)
 8     FORMAT(6E10.4)
 9     FORMAT(2X,10F10.6)
 10    FORMAT(1H1)
 11    FORMAT(///)
 13    FORMAT(10E11.3)
C
C     ***   TRANSPOSE  B AND H
       DO 14 I=1,KK
       DO 14 J=1,NN
  14   HT(J,I)=H(I,J)
C
       CALL  TMAT
       CALL GMPRD(HT,Q,HQ,NN,KK,KK,K2,K1,K2)
       CALL GMPRD(HQ,H,QQ,NN,KK,NN,K2,K2,N2)
       WRITE(6,11)
       WRITE(6,9) ((A(I,J),J=1,NN),I=1,NN)
       WRITE(6,11)
       WRITE(6,3) ((B(I,J),J=1,M),I=1,NN)
       WRITE(6,11)
       WRITE(6,13)((QQ(I,J),J=1,NN),I=1,NN)
C
       DO 15 I=1,NN
       DO 15 J=1,NN
  15   PP(I,J)=QQ(I,J)
       DO 16 I=1,M
       DO 16 J=1,NN
```

```
   16  TT(I,J)=0.1
       DO 17 I=1,NN
       DO 17 J=1,M
   17  BT(J,I)=B(I,J)
C
       CALL GAINS
       WRITE(6,10)
C
C      ***  SOLVE FOR OPTIMAL CONTROL
C         AND TRAJECTORY
C
       WRITE(6,18)
   18  FORMAT(5X,'Q'//)
       WRITE(6,20) ((Q(I,J),J=1,KK),I=1,KK)
       WRITE(6,19)
   19  FORMAT(//)
   20  FORMAT (8X,4E12.3)
       WRITE(6,21)
   21  FORMAT(4X,'X1',11X,'X2',10X,'X3',9X,'X4',9X,'X5',9X,'X6',
      1  10X,'X7',9X,'X8',9X,'U1',9X,'U2')
       IK=0
       A1=0.
       A2=0.
       A3=0.
       IX=9
       DO 29 K=1,400
       DO 23 I=1,M
       U(I)=0.0
       DO 23 J=1,NN
       T(J)=X(J)
   23  U(I)=U(I)+FF(I,J)*X(J)
       CALL GMPRD(A,T,S,NN,NN,1,N2,NN,NN)
```

```
      CALL GMPRD(B ,U,ST,NN,M,1,NNM,M,NN)
      CALL GMADD(S,ST,X,NN,1,NN)
      DO 26 KG=4,K,4
      TIM=K*DT
      IF(KG .EQ. K) GO TO 27
 26   CONTINUE
      GO TO 28
 27   IK=IK+1
      YY(1,IK)=X(1)
      YY(2,IK)=X(5)
      YY(3,IK)=X(2)
      YY(4,IK)=X(6)
      YY(5,IK)=X(3)
      YY(6,IK)=X(7)
      YY(7,IK)=X(4)
      YY(8,IK)=X(8)
      WRITE(6,30) (X(I),I=1,8),(U(I),I=1,M),X(10)
 28   CONTINUE
  29  CONTINUE
  30  FORMAT(1X,10E11.3,4X,F7.4)
C
C
C  ***  SCALING ROUTINE
      NY=1
      NX=2
 70   TMAX=.00010
      TMIN=-.00010
      DO 72 J=1,100
      Y(1,J)=YY(NY,J)
 72   Y(2,J)=YY(NX,J)
      DO 80 I=1,2
      DO 80 IK=1,100
```

```
      TEST=Y(I,IK)
      IF(TEST .GT. TMAX)  TMAX=TEST
      IF(TEST .LT. TMIN)  TMIN=TEST
 80   CONTINUE
      SCALE=ABS(TMAX) + ABS(TMIN)
      TM=90./SCALE
      NS=(100./SCALE)*TMAX
      DO 81 I=1,2
      DO 81 IK=1,100
 81   Y(I,IK)=TM*Y(I,IK)
      WRITE(6,82)  TM
 82   FORMAT(1H1, ' SCALE FACTOR IS TM=',F10.6///)
      CALL PLOT(Y,2,100,NS)
      NY=NY+2
      NX=NX+2
      IF(NX .GT. 8)  GO TO 31
 85   GO TO 70
  31  GO TO 4
  32  STOP
       END
      SUBROUTINE PLOT (Y,KI,NF,NS)
C   SUBROUTINE FOR PLOTTING 5 X 100 INPUT ARRAY (FORTRAN 4)
      DIMENSION Y(2,100), LINE(101),L(11),JL(5)
      DATA(JL(I),I=1,5)/1H*,1H.,1HC,1HD,1HE/,JN,JP,JI,JBLANK,JZ/
     11H-,1H+,1HI,1H ,1H$/
      DO 99 I=1,101
      LINE(I)=JBLANK
 99   CONTINUE
      N=0
C   PRINT ORDINATE SCALE
      DO 101 I=1,11
      L(I)=10*I-110+NS
```

```
101    CONTINUE
       PRINT 105,(L(I),I=1,11)
105    FORMAT(3X,11(I4,6X),6HY(1,I))
       GO TO 115
110    IF(N/10-(N-1)/10) 125,125,115
C   CONSTRUCT ORDINATE GRAPH LINE
115    ND=0
       DO 120 I=1,10
       ND=ND+1
       LINE(ND)=JP
       DO 120 J=1,9
       ND=ND+1
120    LINE(ND)=JN
       LINE(101)=JP
       IF(N) 135,121,135
121    PRINT 170,N,LINE
       GO TO 185
C      CONSTRUCT 1 LINE OF ABSCISSA GRAPH LINES
125    DO 130 I=1,101,10
       LINE(I)=JI
130    CONTINUE
C     CHANGE NUMERICAL DATA TO LETTERS
135    DO 160 I=1,KI
       XNS=NS
       JA=Y(I,N)+101.49999-XNS
       IF(JA-101) 140,155,145
140    IF(JA) 150,150,155
145    LINE(101)=JZ
       GO TO 160
150    LINE(1)=JZ
       GO TO 160
155    LINE(JA)=JL(I)
```

```
160    CONTINUE
C    PRINT LINE OF DATA
       IF (N/10-(N-1)/10) 175,175,165
165    PRINT 170,N,LINE,Y(1,N)
170    FORMAT (1X,I4,101A1,1X,1PE12.5)
       GO TO 185
175    PRINT 180 ,LINE ,Y(1,N)
180    FORMAT (5X,101A1,1X,E12.5)
C     SET LINE VARIABLES TO ZERO
185    DO 190 I=1,101
       LINE(I)=JBLANK
190    CONTINUE
195    N=N+1
       IF(N-NF) 110,110,200
200     RETURN
       END
       SUBROUTINE GAINS
       COMMON AA(12,12),A(10,10),B(10,2),R(2,2),H(4,10),Q(4,4),
      1 QQ(10,10),HQ(10,4),BT(2,10),BTP(2,10),BTPB(2,2),RB(2,2),
      2 RBT(2,10),ADT2(12,12),FF(2,10),PP(10,10),BFF(10,10),
      3 V(10,10),VT(10,10),L(10),E(10),HT(10,4),FFT(10,2),GG,
      4 VTP(10,10),VTPV(10,10),FTR(10,2),EADT2(12,12),FRF(10,10),
      5 TT(2,10),ST(10),X(10),T(10),S(10),U(2),EADT(12,12),
      6 S1(12,12),S2(12,12),N,NN,M,KN,DT,NNM,MM,N2,K1,K2,KK,EE,G,
      7  YY(8,100),Y(2,100),XV(350)
       INTEGER E,GG,G,EE
       WRITE(6,1)
  1    FORMAT(1H1)
       DO 16 K=1,GG
       CALL GMPRD(BT,PP,BTP,M,NN,NN,NNM,N2,NNM)
       CALL GMPRD(BTP,B,BTPB,M,NN,M,NNM,NNM,MM)
       CALL GMADD(R,BTPB,RB,M,M,MM)
```

```
      CALL MINV(RB,M,DET,L,E,MM)
      DO 2 I=1,M
      DO 2 J=1,M
    2 RB(I,J)=-RB(I,J)
      CALL GMPRD(RB,BTP,RBT,M,M,NN,MM,NNM,NNM)
      CALL GMPRD(RBT,A,FF,M,NN,NN,NNM,N2,NNM)
      CALL GMPRD(B,FF,BFF,NN,M,NN,NNM,NNM,N2)
      CALL GMADD(A,BFF,V,NN,NN,N2)
C
C     *** TRANSPOSE  V AND FF
C
      DO 3 I=1,NN
      DO 3 J=1,NN
    3 VT(J,I)=V(I,J)
      DO 4 I=1,M
      DO 4 J=1,NN
    4 FFT(J,I)=FF(I,J)
C
      CALL GMPRD(VT,PP,VTP,NN,NN,NN,N2,N2,N2)
      CALL GMPRD(VTP,V,VTPV,NN,NN,NN,N2,N2,N2)
      CALL GMPRD(FFT,R,FTR,NN,M,M,NNM,MM,NNM)
      CALL GMPRD(FTR,FF,FRF,NN,M,NN,NNM,NNM,N2)
C
C      *** P(K)=VTPV + FRF + Q
      DO 5 I=1,NN
      DO 5 J=1,NN
    5 PP(I,J)=VTPV(I,J) + FRF(I,J) + QQ(I,J)
      DO 6 II=50,KN,50
      IF(K .EQ. II) GO TO 7
    6 CONTINUE
      GO TO 14
    7 CONTINUE
```

```
      WRITE(6,8) K
    8 FORMAT(2X,/4H K= ,I4)
      DO 9 I=1,NN
    9 WRITE(6,11) (PP(I,J),J=1,NN)
      DO 10 I=1,M
   10 WRITE(6,11) (FF(I,J),J=1,NN)
   11 FORMAT(2X,10E12.3)
      IF(K .LT. 50) GO TO 16
C
C     ***  TEST TO SEE IF F IS CONSTANT
C
      G=K-1
      DO 12 I=1,M
      DO 12 J=1,NN
      TEST=(FF(I,J)-TT(I,J))/TT(I,J)
      IF(ABS(TEST) .GT. 1.E-04 ) GO TO 14
   12 CONTINUE
      WRITE(6,13) K
   13 FORMAT(////1H ' F MATRIX IS CONSTANT '/
     11H ' K=',I3//)
      RETURN
   14 DO 15 I=1,M
      DO 15 J=1,NN
   15 TT(I,J)=FF(I,J)
   16 CONTINUE
      RETURN
      END
      SUBROUTINE  TMAT
C     STATE TRANSITION
      COMMON AA(12,12),A(10,10),B(10,2),R(2,2),H(4,10),Q(4,4),
     1 QQ(10,10),HQ(10,4),BT(2,10),BTP(2,10),BTPB(2,2),RB(2,2),
     2 RBT(2,10),ADT2(12,12),FF(2,10),PP(10,10),BFF(10,10),
```

```
     3 V(10,10),VT(10,10),L(10),E(10),HT(10,4),FFT(10,2),GG,
     4 VTP(10,10),VTPV(10,10),FTR(10,2),EADT2(12,12),FRF(10,10),
     5 TT(2,10),ST(10),X(10),T(10),S(10),U(2),EADT(12,12),
     6 S1(12,12),S2(12,12),N,NN,M,KN,DT,NNM,MM,N2,K1,K2,KK,EE,G,
     7  YY(8,100),Y(2,100),XV(350)
      INTEGER E,GG,G,EE
      KN=KN+1
      GG=KN-1
  10  FORMAT(1X,12F10.5)
C     CALCULATION OF EADT2
      DO 15 I=1,N
      DO 15 J=1,N
      EADT2(I,J)=0.0
      S1(I,J)=0.0
      S1(I,I)=1.0
      EADT2(I,I)=1.0
  15  ADT2(I,J)=AA(I,J)*DT*0.5
      KMIN=1
      KMAX=7
  20  CONTINUE
      DO 25 K=KMIN,KMAX
      DO 30 I=1,N
      DO 30 J=1,N
      S2(I,J)=0.0
      DO 30 LL=1,N
  30  S2(I,J)=S2(I,J)+S1(I,LL)*ADT2(LL,J)/FLOAT(K)
      DO 35 I=1,N
      DO 35 J=1,N
      S1(I,J)=S2(I,J)
  35  EADT2(I,J)=EADT2(I,J)+S2(I,J)
  25  CONTINUE
C      CALCULATE RATIO OF NORMS LESS THAN  10**(-6)
```

```
      RNORS2=0.0
      RNORE2=0.0
      DO 40 I=1,N
      DO 40 J=1,N
      RNORS2=RNORS2+ABS(S2(I,J))
   40 RNORE2=RNORE2+ABS(EADT2(I,J))
      IF (RNORE2 .EQ.  0.0) STOP
      TST=RNORS2/RNORE2
      TSTMAX=FLOAT(N)*1.0E-06
      IF(TST .LE. TSTMAX) GO TO 45
      KMIN=KMAX+1
      KMAX=KMAX+3
      GO TO 20
   45 CONTINUE
C
C     CALCULATION OF EADT
C
      DO 50 I=1,N
      DO 50 J=1,N
      EADT(I,J)=0.0
      DO 50 K=1,N
   50 EADT(I,J)=EADT(I,J)+EADT2(I,K)*EADT2(K,J)
      WRITE(6,55)
   55 FORMAT(//)
      WRITE(6,10) ((EADT(I,J),J=1,N),I=1,N)
C     LOAD A AND B FROM EADT
      KM=N-M
      DO 60 I=1,KM
      DO 60 J=1,KM
   60 A(I,J)=EADT(I,J)
      DO 65 J=1,M
      DO 65 I=1,NN
```

```
65   B(I,J)=EADT(I,NN+J)
     RETURN
     END
```

The vita has been removed from the scanned document

A MODEL-FOLLOWING DIGITAL CONTROL LAW FOR AN EBF-STOL AIRCRAFT

by

Reidar Alvestad

(ABSTRACT)

A method is presented for augmenting the control of an EBF-STOL aircraft using a real model-following technique. The method is based on the solution of the discrete matrix Riccati equation to generate the required feedback and feedforward gains. The feedback gains provide a means of closing the control loop around each of the plant states while the feedforward gains multiply the states of the inputs to some desirable reference model, thus making it a prefilter to the plant. The model chosen for this research is that of a B-26 aircraft.

The longitudinal equations of motion of the STOL aircraft are linearized about a preselected point of the flight regime and written as linear state equations. A new system state vector is then constructed which includes the difference between plant and model states. The problem is formulated as a discrete linear regulator with the inputs to the model simulated as state variables.

In solving the matrix Riccati equation, a quadratic cost function which includes the system state vector is minimized, thus making the plant states follow those of the model.

The type of STOL aircraft used in this study has three possible fixed flap positions. Results are obtained for the half-flap

configuration with step inputs to the elevator and thrust coefficient. Results are also presented for a filtered gaussian input to each of these control variables.